JOURNAL OF HEMATOLOGY & ONCOLOGY

LETTER TO THE EDITOR Open Access

8q24 amplified segments involve novel fusion genes between *NSMCE2* and long noncoding RNAs in acute myelogenous leukemia

Yoshiaki Chinen[1†], Natsumi Sakamoto[1†], Hisao Nagoshi[1], Tomohiko Taki[2], Saori Maegawa[1], Shotaro Tatekawa[1], Taku Tsukamoto[1], Shinsuke Mizutani[1], Yuji Shimura[1], Mio Yamamoto-Sugitani[1], Tsutomu Kobayashi[1], Yosuke Matsumoto[1], Shigeo Horiike[1], Junya Kuroda[1*] and Masafumi Taniwaki[1]

Abstract

The pathogenetic roles of 8q24 amplified segments in leukemic cells with double minute chromosomes remain to be verified. Through comprehensive molecular analyses of 8q24 amplicons in leukemic cells from an acute myelogenous leukemia (AML) patient and AML-derived cell line HL60 cells, we identified two novel fusion genes between *NSMCE2* and long noncoding RNAs (lncRNAs), namely, *PVT1-NSMCE2* and *BF104016-NSMCE2*. Our study suggests that 8q24 amplicons are associated with the emergence of aberrant chimeric genes between *NSMCE2* and oncogenic lncRNAs, and also implicate that the chimeric genes involving lncRNAs potentially possess as-yet-unknown oncogenic functional roles.

Keywords: Acute myeloid leukemia (AML), Long noncoding RNAs (lincRNAs), *PVT1*, *NSMCE2*, *CCDC26*

To the Editor,

To gain insight into the role(s) of double minute chromosomes (dmins) in leukemia, we cytogenetically/molecularly analyzed 8q24 amplicons in patient-derived leukemic cells and AML-derived cell line (HL60) (See Additional file 1 for supplementary materials and methods). The patient was a 71-year-old female with AML (M2). The G-banding karyotype of leukemic cells was 47, XX, +mar [2]/48, XX, idem, +mar [6]/46, XX [7], containing two marker chromosomes (mars) from chromosome 8 (Figure 1a and b). DNA copy number analysis (CNA) revealed 13 high-level amplicons on 8q22.1-q24.2 (98.43 Mb-134.16 Mb) (Additional file 2: Table S1). SKY analysis of HL60 cells containing the 8q24 amplicons revealed that the representative karyotype was 44, X, der(5)t(5;17)(q11.2;q11.2), t(7;16;9)(q34;q24;p21), t(9;14)(q22;q22), +13, -15, -17, der(21)t(15;21)(q22;q21) [1]. CNA revealed several amplicons on 8q24.13-q24.12 (126.25 Mb-130.75 Mb) in the HL60 cells (Figure 2a and b). Consequently, three common amplicons were identified between 8q24.13-21 in the patient and the HL60 cells; i.e., the regions covering *NSMCE2* (8q24.13), *PVT1* (8q24.21) and *CCDC26* (8q24.21) (Figures 1c and 2b). Further investigation revealed three fusion transcripts between *PVT1* exon 1a and *NSMCE2* exon 3 in the patient (Figure 1d and e), and a fusion gene between exon 6 of *NSMCE2* and exon 1 of *BF104016*, a noncoding RNA sharing the sequence of *CCDC26* exon 4 (Additional file 3: Figure S1) (Additional file 4: Table S2), in the HL60 cells (Figure 2c-e). Both the *NSMCE2* and *PVT1* genes were amplified and located in a micronucleus in the patient (Figure 1f-i), and the genomic junction of 5'-*PVT1-NSMCE2*-3' was located within intron 1 of *PVT1* and at 5' upstream of exon 1 of *NSMCE2* (Figure 1j and k) (Additional file 5: Figure S3). In the HL60 cells, amplification of 3'*NSMCE2* and 5'*CCDC26* was co-localized on der(13)hsr(8), ins(2;8) and dmins (Figure 2e-h) (Additional file 5: Figure S3). Aberrant *NSMCE2* transcripts were higher than normal *NSMCE2* transcripts in the patient and the HL60 cells, while NSMCE2 protein expression did not correlate with normal or abnormal *NSMCE2* transcripts among the leukemic patient cells or the HL60 cells, suggesting the presence of regulatory mechanisms other than transcription (Additional file 6: Figure S2).

* Correspondence: junkuro@koto.kpu-m.ac.jp
†Equal contributors
[1]Division of Hematology and Oncology, Department of Medicine, Kyoto Prefectural University of Medicine, Graduate School of Medical Science, 465 Kajii-choKamigyo-ku, Kyoto 602-8566, Japan
Full list of author information is available at the end of the article

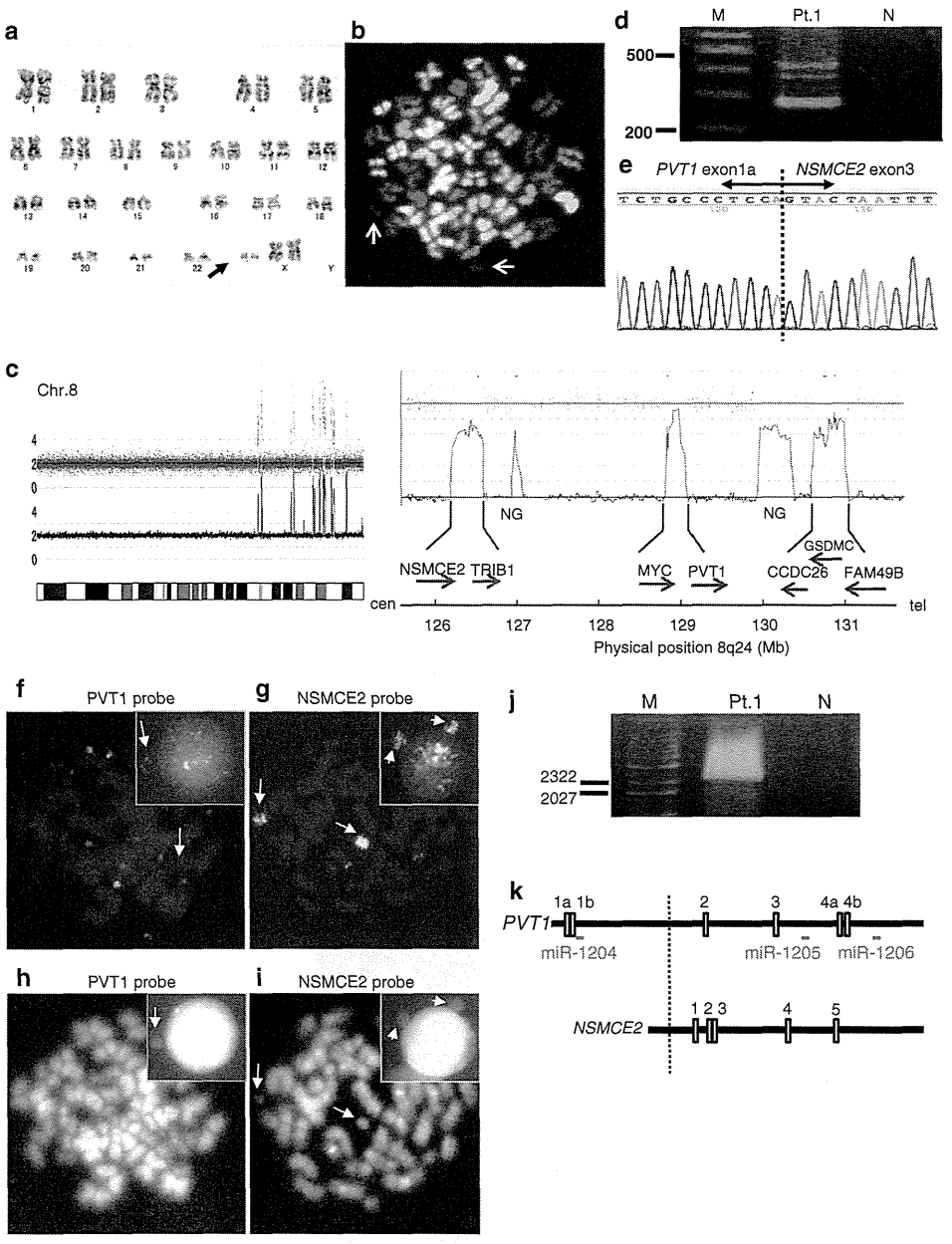

Figure 1 Identification of *PVT1-NSMCE2* in the leukemic patient cells. (a) G-banding analysis. Arrow indicates two marker chromosomes (mars). **(b)** SKY analysis for the patient identified two mars derived from chromosome 8 (arrows). **(c)** Copy number changes at 8q24 detected by high-resolution oligonucleotide array. *NSMCE2*, *TRIB1*, *MYC*, *PVT1*, *CCDC26*, *GSDMC*, and *FAM49B* are amplified. The direction of the arrows reflects the direction of gene transcription. NG: no gene. **(d)** Detection of three *PVT1-NSMCE2* fusion transcripts by RT-PCR. Primers were P1S and NSMCE2-Ex4AS for 5'-PVT1-NSMCE2-3'. Lane Pt.1: leukemic cells from the patient; lane N: water; lane M: size marker. **(e)** Sequence analysis of *NSMCE2* fusion transcript in the patient. **(f)** FISH finding of the patient using *PVT1* probe. Multiple red signals indicate extrachromosomal amplification of *5'PVT1* on dmins. Co-localized red and green signals indicate normal *PVT1*. Inset shows *5'PVT1* amplification in a micronucleus equivalent of mar (arrow). (Additional file 5: Figure S3) **(g)** FISH finding from the patient using an *NSMCE2* probe. Intense yellow signals indicate amplification of *NSMCE2* on mars and co-localized red and green signals signify normal *NSMCE2* on chromosome 8. Inset shows *NSMCE2* amplification in a micronucleus equivalent of mar (arrow). **(h** and **i)** DAPI pictures of metaphase cells corresponding to **(f)** and **(g)**. Arrows indicate mars. In metaphase, *NSMCE2* amplification was detectable on mars. *5'PVT1* amplification were observed on dmins, however, *PVT1* FISH probe sets could not identify mars because of the background dmins (f and h). **(j)** Results of LDI-PCR. Primers were NSM38374 and NSM38666 for 5'-PVT1-NSMCE2-3'. Lane Pt.1: leukemic cells from the patient; lane N: water; lane M: size marker. (Additional file 4: Table S2) **(k)** Genomic mapping of *PVT1* and *NSMCE2* exons and breakpoint. White vertical boxes represent exons; dotted line represents breakpoint of *PVT1* and *NSMCE2* in the patient detected by LDI-PCR. Horizontal line indicates the location of miRNAs.

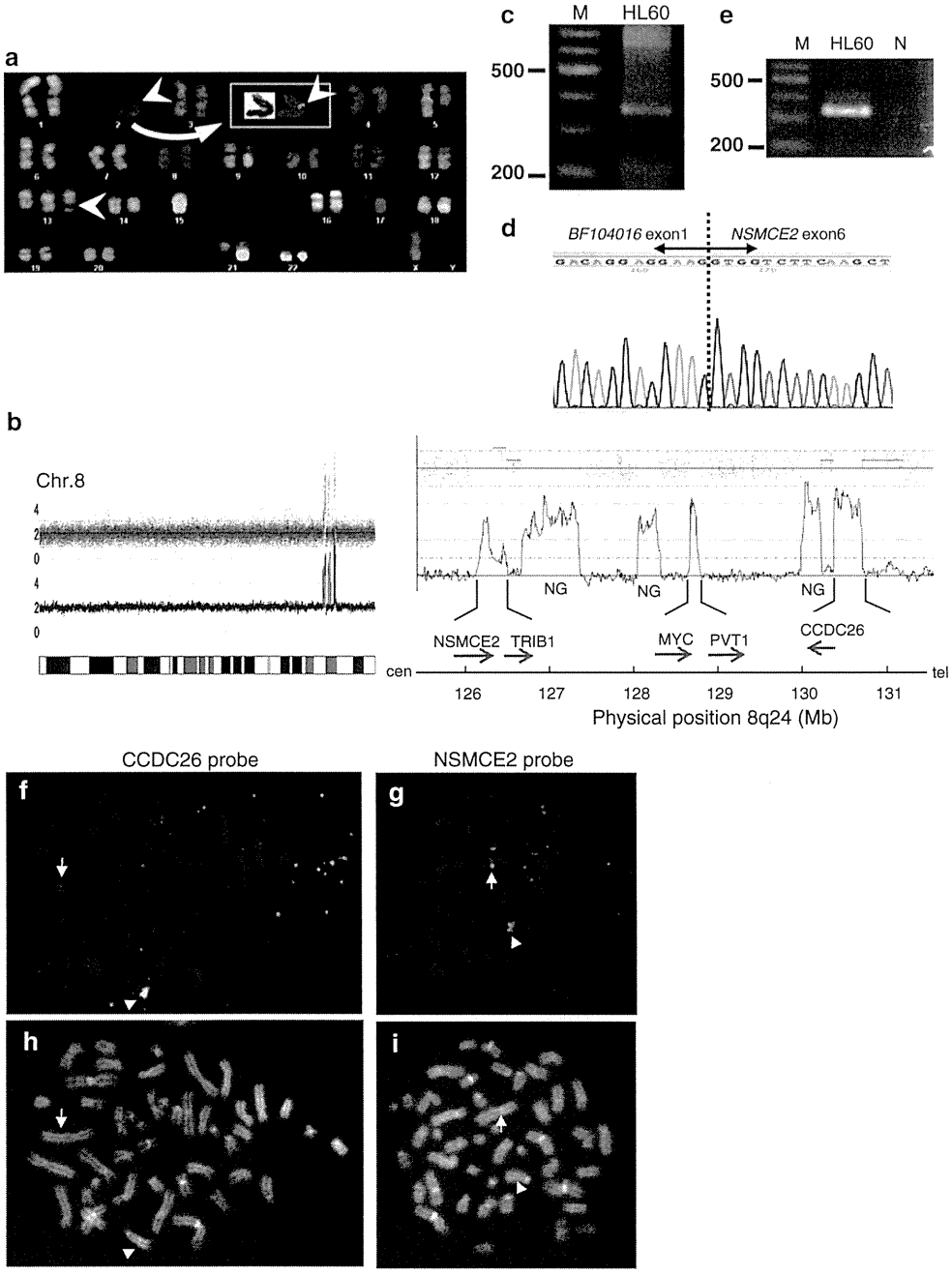

Figure 2 Identification of *BF104016-NSMCE2* in HL60. (a) Representative SKY karyotype of HL60 cells. Arrowheads indicate material inserted from chromosome 8 on ins(2;8) and der(13)hsr(8). Inset shows pseudocolor image of ins(2;8). **(b)** Copy number changes at 8q24 detected by high-resolution oligonucleotide array. *NSMCE2*, *TRIB1*, *MYC*, *PVT1* and *CCDC26* are amplified in HL60. The direction of the arrows reflects the direction of the gene transcription. NG: no gene. **(c)** Bubble PCR products detected by nested PCR using NVAMP1 and NSMCE2-Ex7AS for the first PCR, and NVAMP2 and NSM695 for the second. M: size marker. **(d)** Sequence analysis of *NSMCE2* fusion transcript of HL60. **(e)** Detection of *BF104016-NSMCE2* fusion transcripts by RT-PCR. Primers were BF104-1S and NSMCE2-Ex7AS for 5'-BF104016-NSMCE2-3'. Lanes N: water. (Additional file 4: Table S2) **(f)** FISH finding of HL60 using *CCDC26* probe. Intense co-localized red and green signal indicates amplification of the *CCDC26* gene on der(13)hsr(8) (arrowhead). A co-localized red and green signal is seen on ins(2;8) (arrow). Multiple green signals indicate amplification of the *5'CCDC26* gene on dmins. Co-localized red and green signals show normal *CCDC26*. **(g)** FISH finding of HL60 using *NSMCE2* probe. Intense green signals indicate amplification of *3'NSMCE2* on der(13)hsr(8) (arrowhead) and ins(2;8) (arrow). Multiple red and green signals indicate amplification of the *NSMCE2* gene on dmins. Co-localized red and green signals indicate normal chromosomal *NSMCE2*. (Additional file 5: Figure S3) **(h** and **i)** DAPI pictures of metaphase cells corresponding to **(f)** and **(g)**. Arrow and arrowhead indicate ins(2;8) and der(13)hsr(8), respectively.

The present findings are consistent with previous studies demonstrating that segmental genome amplification of 8q24 contains recurrent *PVT1* fusion genes, which might be generated by chromothripsis [2,3]. Both lncRNAs, *PVT1* and *CCDC26,* harbor retroviral integration sites and are transcribed into multiple splice forms [4-6]. *PVT1* overexpression is induced by *MYC* or p53, contributing to suppression of apoptosis [7-9], whereas *PVT1* produces six annotated microRNAs that have been implicated in oncogenesis [3,10,11]. The chimeric transcripts involving *PVT1* may also regulate the expression of as-yet unspecified target genes through "enhancer-like functions" [12]. *CCDC26* amplification has been also identified as a recurrent abnormality that is associated with the response to retinoic acid-induced differentiation in AML [1,11,13-16]. This study is the first to identify *NSMCE2*-associated fusion genes in AML [17-19]. Knockdown of *NSMCE2* induces chromosomal instability and increases the frequency of chromosomal breakage and loss [20]. We speculate that *NSMCE2* gene rearrangement may potentially influence its function. Collectively, our study identified novel *PVT1-NSMCE2* and *CCDC26-NSMCE2* fusion genes that may play functional roles in leukemia.

Additional files

Additional file 1: Supplementary material information.

Additional file 2: Table S1. CNAG analysis of the region between the *MTDH* and *LRRC6* genes on 8q24 in patient 1 with marker chromosomes. Results show the genomic size of the eight amplified segments that were selected based on the existence of known genes within them and their approximate positions.

Additional file 3: Figure S1. Association between *CCDC26* and *BF104016* at 8q24.21. The scale indicates the region 8q24.21. White boxes and grey boxes indicate exons of *CCDC26* and *BF104016* on the genetic locus at 8q24.21, respecitively. Vertical black lines indicate exons on the *CCDC26* isoform. According to the NCBI database, isoform 1 (BC070152.1) consists of four (1-2-3-4) exons, and isoform 2 (BC026098.1) consists of three (1a-3-4) exons. *BF104016* consists of 2 exons. The sequence of *BF104016* exon 2 is partly consistent with that of *CCDC26* exon 4. ORF: hypothetical open reading frame.

Additional file 4: Table S2. Sequences of the primers used in this study.

Additional file 5: Figure S3. Identification of breakpoints region at 8q24 by FISH. Upper panel: location of FISH probes shown as color bars and position of *NSMCE2*, *TRIB1*, *MYC*, and *PVT1* genes at 8q24. Vertical black lines indicate exons of *NSMCE2*, *PVT1*, and *BF104016*. Lower panel: mapping of breakpoint in leukemic cells of patient 1 and HL60. Gray boxes indicate amplified regions detected.

Additional file 6: Figure S2. Expression of *NSMCE2* in patient 1 and AML-derived cell lines. (a) *NSMCE2* mRNA levels measured by RQ-PCR (n=3, mean ± SD). Theoretically, the NSMCE2 7-8 primer/probe can amplify both normal and aberrant *NSMCE2* transcripts, while the NSMCE2 2-3 primer/probe set which can amplify only normal *NSMCE2* transcript. *NSMCE2* mRNA levels were normalized to β-actin and are relative to the control mRNA extracted from normal BM cells. *NSMCE2* mRNA levels amplified by the NSMCE2 7-8 primer/probe set are higher than those amplified by the NSMCE2 2-3 primer/probe set in patient 1, HL60 and KG1 cells. (b) Protein analysis using the anti-NSMCE2 antibody in cells. Blot for β-actin was used as loading control. Lane 1: normal BM; lane 2: KG1; lane 3: HL60. (c and d) IHC analysis of NSMCE2 expression in BM of patient 1 (c) and normal BM (d). NSMCE2 expression of leukemic cells was not higher than that of normal BM cells. Monocytes and megakaryocytes showed strong positive signals in their cytoplasm.

Abbreviations

dmins: Double minute chromosomes; hsr: Homogeneously staining regions; FISH: Fluorescence *in situ* hybridization; lncRNAs: Long noncoding RNAs; AML: Acute myeloid leukemia; MDS: Myelodysplastic syndromes; NSMCE2: Non-SMC element 2; SKY: Spectral karyotyping; RT-PCR: Reverse transcription-polymerase chain reaction; LDI-PCR: Long-distance inverse PCR.

Competing interests

The authors declare that they have no competing interests.

Authors' contributions

YC, JK and MT reviewed the literature and wrote the paper. YC, MYS, SM, and SH treated the patient. NS, HN, TT, SM, ST, TT, YS, TK, YM and MT collected the data. YC and NS performed the molecular analyses. YC, JK and MT contributed to the design of this study, final data analysis and edited the manuscript. All authors read and approved the final manuscript.

Acknowledgements

The authors thank Akari Kazami and Yoko Yamane for their expert technical assistance. This study was performed as a research program of the Project for Development of Innovative Research on Cancer Therapeutics (P-Direct), Ministry of Education, Culture, Sports, Science and Technology of Japan, and supported by a Grant-in-Aid for Cancer Research from the Ministry of Health, Labor and Welfare of Japan, by a Grant-in-aid for Scientific Research (B) and (C) from the Ministry of Education, Culture, Sports, Science and Technology of Japan, and by the National Cancer Center Research and Development Fund.

Author details

[1]Division of Hematology and Oncology, Department of Medicine, Kyoto Prefectural University of Medicine, Graduate School of Medical Science, 465 Kajii-choKamigyo-ku, Kyoto 602-8566, Japan. [2]Department of Molecular Diagnostics and Therapeutics, Kyoto Prefectural University of Medicine, Graduate School of Medical Science, Kyoto, Japan.

Received: 2 September 2014 Accepted: 11 September 2014
Published online: 23 September 2014

References

1. Hirano T, Ike F, Murata T, Obata Y, Utiyama H, Yokoyama KK: **Genes encoded within 8q24 on the amplicon of a large extrachromosomal element are selectively repressed during the terminal differentiation of HL-60 cells.** *Mutat Res* 2008, **640**:97–106.
2. Campbell PJ, Stephens PJ, Pleasance ED, O'Meara S, Li H, Santarius T, Stebbings LA, Leroy C, Edkins S, Hardy C, Teague JW, Menzies A, Goodhead I, Turner DJ, Clee CM, Quail MA, Cox A, Brown C, Durbin R, Hurles ME, Edwards PA, Bignell GR, Stratton MR, Futreal PA: **Identification of somatically acquired rearrangements in cancer using genome-wide massively parallel paired-end sequencing.** *Nat Genet* 2008, **40**:722–729.
3. Northcott PA, Shih DJ, Peacock J, Garzia L, Morrissy AS, Zichner T, Stütz AM, Korshunov A, Reimand J, Schumacher SE, Beroukhim R, Ellison DW, Marshall CR, Lionel AC, Mack S, Dubuc A, Yao Y, Ramaswamy V, Luu B, Rolider A, Cavalli FM, Wang X, Remke M, Wu X, Chiu RY, Chu A, Chuah E, Corbett RD, Hoad GR, Jackman SD, *et al*: **Subgroup-specific structural variation across 1,000 medulloblastoma genomes.** *Nature* 2012, **488**:49–56.
4. Graham M, Adams JM, Cory S: **Murine T lymphomas with retroviral inserts in the chromosomal 15 locus for plasmacytoma variant translocations.** *Nature* 1985, **314**:740–743.
5. Lemay G, Jolicoeur P: **Rearrangement of a DNA sequence homologous to a cell-virus junction fragment in several Moloney murine leukemia virus-induced rat thymomas.** *Proc Natl Acad Sci USA* 1984, **81**:38–42.
6. Villeneuve L, Rassart E, Jolicoeur P, Graham M, Adams JM: **Proviral integration site Mis-1 in rat thymomas corresponds to the pvt-1 translocation breakpoint in murine plasmacytomas.** *Mol Cell Biol* 1986, **6**:1834–1837.

7. Guan Y, Kuo WL, Stilwell JL, Takano H, Lapuk AV, Fridlyand J, Mao JH, Yu M, Miller MA, Santos JL, Kalloger SE, Carlson JW, Ginzinger DG, Celniker SE, Mills GB, Huntsman DG, Gray JW: **Amplification of PVT1 contributes to the pathophysiology of ovarian and breast cancer.** *Clin Cancer Res* 2007, **13**:5745–5755.
8. Carramusa L, Contino F, Ferro A, Minafra L, Perconti G, Giallongo A, Feo S: **The PVT-1 oncogene is a Myc protein target that is overexpressed in transformed cells.** *J Cell Physiol* 2007, **213**:511–518.
9. Barsotti AM, Beckerman R, Laptenko O, Huppi K, Caplen NJ, Prives C: **p53-Dependent induction of PVT1 and miR-1204.** *J Biol Chem* 2012, **287**:2509–2519.
10. Beck-Engeser GB, Lum AM, Huppi K, Caplen NJ, Wang BB, Wabl M: **Pvt1-encoded microRNAs in oncogenesis.** *Retrovirology* 2008, **5**:4.
11. Huppi K, Volfovsky N, Runfola T, Jones TL, Mackiewicz M, Martin SE, Mushinski JF, Stephens R, Caplen NJ: **The identification of microRNAs in a genomically unstable region of human chromosome 8q24.** *Mol Cancer Res* 2008, **26**:212–221.
12. Ørom UA, Derrien T, Beringer M, Gumireddy K, Gardini A, Bussotti G, Lai F, Zytnicki M, Notredame C, Huang Q, Guigo R, Shiekhattar R: **Long noncoding RNAs with enhancer-like function in human cells.** *Cell* 2010, **143**:46–58.
13. Radtke I, Mullighan CG, Ishii M, Su X, Cheng J, Ma J, Ganti R, Cai Z, Goorha S, Pounds SB, Cao X, Obert C, Armstrong J, Zhang J, Song G, Ribeiro RC, Rubnitz JE, Raimondi SC, Shurtleff SA, Downing JR: **Genomic analysis reveals few genetic alterations in pediatric acute myeloid leukemia.** *Proc Natl Acad Sci USA* 2009, **106**:12944–12949.
14. Guttman M, Amit I, Garber M, French C, Lin MF, Feldser D, Huarte M, Zuk O, Carey BW, Cassady JP, Cabili MN, Jaenisch R, Mikkelsen TS, Jacks T, Hacohen N, Bernstein BE, Kellis M, Regev A, Rinn JL, Lander ES: **Chromatin signature reveals over a thousand highly conserved large non-coding RNAs in mammals.** *Nature* 2009, **458**:223–227.
15. Kühn MW, Radtke I, Bullinger L, Goorha S, Cheng J, Edelmann J, Gohlke J, Su X, Paschka P, Pounds S, Krauter J, Ganser A, Quessar A, Ribeiro R, Gaidzik VI, Shurtleff S, Krönke J, Holzmann K, Ma J, Schlenk RF, Rubnitz JE, Döhner K, Döhner H, Downing JR: **High-resolution genomic profiling of adult and pediatric core-binding factor acute myeloid leukemia reveals new recurrent genomic alterations.** *Blood* 2012, **119**:e67–75.
16. Yin W, Rossin A, Clifford JL, Gronemeyer H: **Co-resistance to retinoic acid and TRAIL by insertion mutagenesis into RAM.** *Oncogene* 2006, **25**:3735–3744.
17. Brown J, Bothma H, Veale R, Willem P: **Genomic imbalances in esophageal carcinoma cell lines involve Wnt pathway genes.** *World J Gastroenterol* 2011, **17**:2909–2923.
18. Parisi F, Ariyan S, Narayan D, Bacchiocchi A, Hoyt K, Cheng E, Xu F, Li P, Halaban R, Kluger Y: **Detecting copy number status and uncovering subclonal markers in heterogeneous tumor biopsies.** *BMC Genomics* 2011, **12**:230.
19. Camps J, Nguyen QT, Padilla-Nash HM, Knutsen T, McNeil NE, Wangsa D, Hummon AB, Grade M, Ried T, Difilippantonio MJ: **Integrative genomics reveals mechanisms of copy number alterations responsible for transcriptional deregulation in colorectal cancer.** *Genes Chromosomes Cancer* 2009, **48**:1002–1017.
20. Rai R, Varma SP, Shinde N, Ghosh S, Kumaran SP, Skariah G, Laloraya S: **Small ubiquitin-related modifier ligase activity of Mms21 is required for maintenance of chromosome integrity during the unperturbed mitotic cell division cycle in Saccharomyces cerevisiae.** *J Biol Chem* 2011, **286**:14516–14530.

doi:10.1186/s13045-014-0068-2
Cite this article as: Chinen *et al.*: 8q24 amplified segments involve novel fusion genes between *NSMCE2* and long noncoding RNAs in acute myelogenous leukemia. *Journal of Hematology & Oncology* 2014 7:68.

bjh research paper

Allogeneic haematopoietic stem cell transplantation for infant acute lymphoblastic leukaemia with *KMT2A (MLL)* rearrangements: a retrospective study from the paediatric acute lymphoblastic leukaemia working group of the Japan Society for Haematopoietic Cell Transplantation

Motohiro Kato,[1,2] Daiichiro Hasegawa,[3] Katsuyoshi Koh,[4] Keisuke Kato,[5] Junko Takita,[1] Jiro Inagaki,[6] Hiromasa Yabe,[7] Hiroaki Goto,[8] Souichi Adachi,[9] Akira Hayakawa,[10] Yasufumi Takeshita,[11] Akihisa Sawada,[12] Yoshiko Atsuta[13,14] and Koji Kato[15]

[1]Department of Paediatrics, The University of Tokyo, [2]Department of Cell Therapy and Transplantation Medicine, The University of Tokyo, Tokyo, [3]Department of Haematology Oncology, Hyogo Children's Hospital, Kobe, [4]Department of Haematology/Oncology, Saitama Children's Medical Centre, Saitama, [5]Department of Haematology/Oncology, Ibaraki Children's Hospital, Mito, [6]Department of Paediatrics, National Kyushu Cancer Centre, Fukuoka, [7]Department of Cell Transplantation and Regenerative Medicine, Tokai University, Isehara, [8]Division of Haematooncology/Regeneration Medicine, Kanagawa Children's Medical Centre, Yokohama, [9]Department of Human Health Sciences, Kyoto University, Kyoto, [10]Department of Paediatrics, Kobe University, Kobe, [11]Department of Paediatrics, Nara Medical University, Kashihara, [12]Department of Haematology/Oncology, Osaka Medical Centre and Research Institute for Maternal and Child Health, Izumi, [13]Japanese Data Centre for Haematopoietic Cell Transplantation, [14]Department of Healthcare Administration, Nagoya University Graduate School of Medicine, Nagoya, and [15]Department of Haematology and Oncology, Children's Medical Centre, Japanese Red Cross Nagoya First Hospital, Nagoya, Japan

Received 15 June 2014; accepted for publication 11 September 2014

Correspondence: Motohiro Kato, 7-3-1, Hongo, Bunkyo-ku, Tokyo 113-8655, Japan.
E-mail: katom-tky@umin.ac.jp

Summary

Allogeneic haematopoietic stem cell transplantation (HSCT) is still considered to play an important role as a consolidation therapy for high-risk infants with acute lymphoblastic leukaemia (ALL). Here, we retrospectively analysed outcomes of HSCT in infants with ALL based on nationwide registry data of the Japan Society for Haematopoietic Cell Transplantation. A total of 132 allogeneic HSCT for infant ALL with *KMT2A (MLL)* gene rearrangements, which were performed in first complete remission (CR1), were analysed. The 5-year overall survival rate after transplantation was 67·4 ± 4·5%). Although recent HSCT (after 2004) had a trend toward better survival, no statistical correlation was observed between outcomes and each factor, including age at diagnosis, initial leucocyte count, cytogenetics, donor types or conditioning of HSCT. Myeloablative conditioning with total body irradiation did not provide a better survival (60·7 ± 9·2%) over that with busulfan (BU; 67·8 ± 5·7%). Two of the 28 patients treated with irradiation, but none of the 90 BU-treated patients, developed a secondary malignant neoplasm. In conclusion, allogeneic HSCT using BU was a valuable option for infant ALL with *KMT2A* rearrangements in CR1.

Keywords: infant, acute lymphoblastic leukaemia, stem cell transplantation, busulfan, total body irradiation.

First published online 10 October 2014
doi: 10.1111/bjh.13174

Although recent advances have achieved excellent cure rates in most cases of paediatric acute lymphoblastic leukaemia (ALL) (Inaba *et al*, 2013), infants with *KMT2A* (*MLL*) rearrangements have worse outcomes than older children (Rubnitz *et al*, 1999; Pui *et al*, 2002; Hilden *et al*, 2006) or infants without *KMT2A* rearrangements (Nagayama *et al*, 2006). Previous clinical studies have reported improvements in the outcomes of infants with ALL characterized by *KMT2A* rearrangements using intensified treatments and allogeneic haematopoietic stem cell transplantation (HSCT) (Silverman *et al*, 1997; Kosaka *et al*, 2004; Jacobsohn *et al*, 2005; Sanders *et al*, 2005; Tomizawa *et al*, 2007), and recent international studies revealed that low-risk infants with ALL could be treated without HSCT, whereas high-risk infants still require allogeneic HSCT as a consolidation therapy (Pieters *et al*, 2007; Mann *et al*, 2010; Dreyer *et al*, 2011). However, optimal allogeneic HSCT strategies, such as the best stem cell source or conditioning regimen, have yet to be determined mainly because of the rarity of infants with ALL.

The high relapse risk of infant ALL with *KMT2A* rearrangements is well known; therefore, allogeneic HSCT at first complete remission (CR1) was indicated for these patients from the second half of 1990s in Japan (Kosaka *et al*, 2004; Tomizawa *et al*, 2007). In the present study, we retrospectively analysed HSCT for infants with ALL based on nationwide registry data of the Japan Society for Haematopoietic Cell Transplantation (JSHCT) in order to obtain fundamental information for establishing a standard approach for infants with ALL.

Patients and methods

This study was approved by the Institutional Ethics Committee of the University of Tokyo Hospital. A total of 132 patients were analysed based on data reported to the JSHCT registry (Atsuta *et al*, 2007). The patients were selected according to the following criteria: (i) diagnosed as ALL with *KMT2A* rearrangements when aged < 1 year old; (ii) allogeneic HSCT was performed in CR1; (iii) HSCT was performed between 1996 and 2011.

The overall survival (OS) probability was calculated using Kaplan–Meier estimates. The duration of event-free survival (EFS) was defined as the time from HSCT to either treatment failure (relapse, death, or the diagnosis of secondary cancer) or to the latest day that the patient was confirmed to be alive. Cumulative incidence curves were used in a competing-risk setting to calculate the probability of engraftment, graft-*versus*-host disease (GVHD) and non-relapse mortality (NRM). Univariate analyses of OS were performed using the log-rank test, and Gray's test was used for group comparisons of cumulative incidences. Engraftment was defined as the first day of three consecutive days with an absolute neutrophil count $\geq 0{\cdot}5 \times 10^9$/l. Myeloablative conditioning was defined as total body irradiation (TBI) of 8 Gy or more, or the administration of busulfan (BU) at a dose higher than 8 mg/kg. All other regimens were analysed as non-myeloablative conditioning (Bacigalupo *et al*, 2009). Multivariate analysis was performed using the Cox proportional-hazard regression model. Univariate analysis did not find any statistical significance ($P < 0{\cdot}2$) between survival outcome and each factor except transplantation period, and the variables considered as clinically important were the patient's age at diagnosis, leucocyte count at diagnosis, the partner gene of the *KMT2A* fusion, donor type and conditioning regimen.

All statistical analyses were performed using R software 2·13·0 (The R Foundation for Statistical Computing, Vienna, Austria).

Results

Patients

All patients and transplantation characteristics are listed in Table I. The median age at diagnosis was 4 months. The median time from the diagnosis to HSCT was 148 days. The median follow-up period after HSCT was 4·9 years (range, 0–16·6 years).

The estimated OS and standard error (±SD) at 5 years after HSCT was 67·4 ± 4·5%. For the 132 patients who underwent HSCT in CR1, the EFS, relapse incidence and NRM were 53·9 ± 4·6%, 34·1 ± 4·4% and 12·0 ± 2·9%, respectively. Fifteen patients died without relapse from various causes: pulmonary complications ($n = 6$), infections ($n = 5$), GVHD ($n = 3$) and sinusoidal obstruction syndrome (SOS) ($n = 1$).

Outcomes of HSCT

The relationships between the outcomes of HSCT according to risk factor are shown in Table II. NRM of HSCT in the recent period (after 2004) was lower than that before 2003 (5·6 ± 2·8% and 20·8 ± 5·6%, respectively), but relapse of the surviving patients minimized the difference in OS (70·8 ± 6·3% and 60·3 ± 6·7%, respectively). Age at diagnosis, initial leucocyte count and partner genes of *KMT2A* rearrangements did not have a prognostic impact on OS, relapse rate or NRM (Figure S1). Thirty-two patients had an initial leucocyte count of 300 × 10^9/l or more, and the OS and EFS of these patients (74·3 ± 8·6% and 51·9 ± 9·9% at 5 years, respectively) were not inferior to those of the other patients.

Conditioning of HSCT

The OS following myeloablative conditioning with BU was 67·8 ± 5·7% ($n = 90$), and the OS with myeloablative TBI was 60·7 ± 9·2% ($n = 28$) (Table II, Fig 1B). Most patients received a combination of etoposide (VP16) and cyclophosphamide (CY) in these myeloablative regimens. Hepatic Sinusoidal obstruction syndrome was observed in 16 of 90 (17·8%) BU patients and three of 28 (10·7%) TBI patients.

Table I. Patient and transplantation characteristics.

Characteristics	Disease status at transplantation First remission
All patients, *n*	132
Transplantation period	
1996–2003	53
2004–2011	79
Age at diagnosis, months	
<3	28
3–5	56
6–12	48
Median initial leucocyte count, × 10^9/l	
<100	59
100–299	28
≥300 000	32
Not known	13
Cytogenetics, *n*	
KMT2A rearrangements	132
t(4;11)/*KMT2A-AFF1*	79
t(9;11)/*KMT2A-MLLT3*	10
t(11;19)/*KMT2A-MLLT1*	10
Other *KMT2A*	33
Others/not known	–
Transplantation donor, *n*	
Related	30
HLA-matched	15
HLA-mismatched	15
Unrelated	13
HLA-matched	12
HLA-mismatched	1
Cord blood	89
HLA-matched	35
HLA-mismatched	54
Transplantation conditioning, *n*	
Myeloablative busulfan	90
VP16+CY	85
Others/not known	5
Myeloablative TBI	28
VP16+CY	19
Others/not known	9
Non-myeloablative	3
Not known	11

HLA, human leucocyte antigen; TBI, total body irradiation; VP16, etoposide; CY, cyclophosphamide.

Although two out of 28 (7·1%) patients who received HSCT with TBI developed thyroid carcinoma as a secondary neoplasm (9·6 and 11·7 years after HSCT), these patients were alive 1·3 and 4·3 years after this diagnosis. In contrast, no secondary neoplasm occurred in the 90 patients that received myeloablative BU or non-myeloablative HSCT (P = 0·05, Fisher's exact test).

Stem cell sources of HSCT in CR1

The stem cell sources of HSCT did not have a significant impact on OS (Table II, Fig 2A). All related donors and unrelated donors achieved engraftment, with a median of 14·5 and 18 days after HSCT. Of 54 cord blood (CB) transplants, 48 achieved engraftment in a median of 18 days, and the engraftment probability was 93·3 ± 2·8% at day 60. The incidence of acute GVHD was slightly higher with unrelated donors (53·8 ± 14·7% at day 100, Fig 2B) than with related donors (28·6 ± 8·7%) and cord blood (29·4 ± 5·0%) (P-value by the log-rank test between unrelated donor and others was 0·05). Among 123 patients who were alive at 100 days after HSCT, chronic GVHD was observed in 6 (21·4%) of 28 transplanted from a related donor, 5 (41·7%) of 12 transplanted from a unrelated donor, and 15 (18·1%) of 83 transplanted with cord blood.

A total of 30 HSCT performed in CR1 was from a related donor, 15 of which were human leucocyte antigen (HLA)-mismatched. Of the 15 mismatched donors, 3 donors were 2- or 3-antigen-mismatched related donors in the graft-*versus*-host (GVH) direction. The HLA disparity among HSCT from related donors did not have a significant difference on outcomes. The 5-year OS of matched related donors was 50·0 ± 13·7%, whereas that of mismatched related donors was 78·0 ± 11·4% (P = 0·20).

Of 89 HLA-mismatched CB, 48 were 1-antigen-mismatched, while 6 were 2- or 3-antigen mismatched. However, mismatched CB was not associated with OS (76·6 ± 8·8% at 5 years for matched CB, 64·6 ± 7·8% for 1-antigen-mismatched CB, and 83·3 ± 15·2% for 2- or 3-antigen-mismatched CB, P = 0·68) (Fig 2C). Status of killer immunoglobulin-like receptor (KIR) ligand incompatibility was identified in 74 HSCT, including 9 KIR ligand mismatches; however, no significant differences were observed when the survival curve of the mismatched group was superimposed on the matched group (P = 0·70, Fig 2D).

The results of multivariate analysis were consistent with those of univariate analysis. Age at diagnosis, initial leucocyte count, partner of the *KMT2A* gene, conditioning regimen and stem cell source did not show significant correlation with survival (Table III). However, recent SCT (after 2004) had a trend toward lower mortality risk although the difference did not reach statistical significance.

Discussion

Although recent large studies reported that intensified chemotherapy without HSCT could provide non-inferior outcomes for relatively low-risk infants with ALL (Pieters *et al*, 2007; Dreyer *et al*, 2011), allogeneic HSCT is still a valuable option for infants with ALL; therefore, an optimal allogeneic HSCT treatment strategy needs to be established. In the present study, in which an analysis of the registry data of the JSCHT was conducted, disease status was the only prognostic factor for OS that was identified in allogeneic HSCT for infants with ALL, and allogeneic HSCT in CR1 could provide similar outcomes independent of the age at diagnosis, initial leucocyte count, partner genes of *KMT2A* rearrangements, stem cell source or conditioning regimen.

Table II. Outcome of HSCT in CR1.

Characteristics	CI of relapse (at 5 years)	*P*	CI of NRM (at 5 years)	*P*	OS (at 5 years)	*P*
All patients	34·1 ± 4·4		12·0 ± 2·9		67·4 ± 4·5	
Transplantation period						
1996–2003	24·5 ± 6·0	0·08	20·8 ± 5·6	0·02	60·3 ± 6·7	0·05
2004–2011	41·9 ± 6·2		5·6 ± 2·8		70·8 ± 6·3	
Age at diagnosis (months)						
<3	39·4 ± 10·1	0·91	11·5 ± 6·4	0·92	74·1 ± 9·3	0·75
3–5	29·4 ± 6·5		13·4 ± 4·8		64·6 ± 6·9	
6–12	36·5 ± 7·5		10·7 ± 4·6		66·9 ± 7·4	
Initial leucocyte count ($\times 10^9$/l)						
<100	30·9 ± 6·4	0·42	7·0 ± 3·4	0·26	75·2 ± 6·1	0·25
≥100	39·9 ± 6·9		14·3 ± 4·7		64·2 ± 7·0	
Cytogenetics						
t(4;11)	29·8 ± 5·5	0·34	13·7 ± 5·5	0·68	64·1 ± 5·7	0·66
t(9;11)	41·6 ± 17·3		0·0 ± 0·0		65·6 ± 20·9	
t(11;19)	38·0 ± 19·6		20·0 ± 13·4		80·0 ± 12·7	
Other *KMT2As*	41·0 ± 9·0		9·4 ± 5·2		70·2 ± 9·3	
Transplantation donor						
Related	40·0 ± 9·7	0·95	13·8 ± 6·5	0·88	63·6 ± 9·3	0·71
Unrelated	15·4 ± 10·5		7·7 ± 7·7		76·9 ± 11·7	
Cord blood	35·2 ± 5·4		12·0 ± 3·6		66·7 ± 5·7	
Transplantation conditioning						
Myeloablative BU	38·9 ± 5·6	0·17	9·6 ± 3·2	0·09	67·8 ± 5·7	0·26
Myeloablative TBI	21·4 ± 7·9		21·4 ± 7·9		60·7 ± 9·2	

HSCT, haematopoietic stem cell transplantation; CR1, first complete remission; CI, cumulative incidence; NRM, non-relapse mortality; OS, overall survival; BU, busulfan; TBI, total body irradiation.

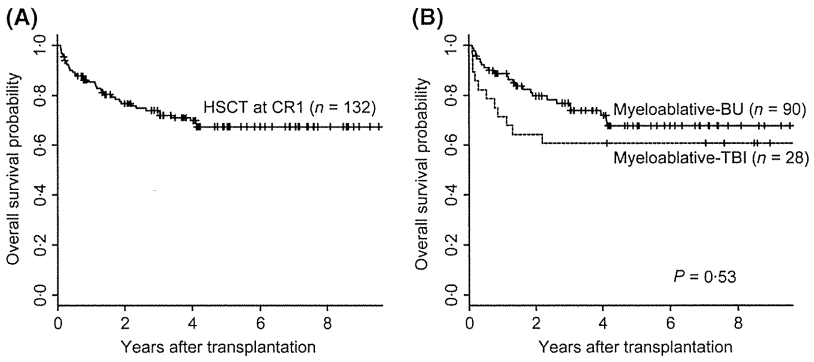

Fig 1. Overall survival following haematopoietic stem cell transplantation. Overall survival probability of (A) all the 132 patients and (B) according to conditioning regimen. BU, busulfan; TBI, total body irradiation.

Recent large studies demonstrated that younger age at diagnosis and higher initial leucocyte count were risk factors for relapse when patients were treated with intensified chemotherapy (Hilden *et al*, 2006; Pieters *et al*, 2007; Dreyer *et al*, 2011). Our results showed that the outcome of HSCT in CR1 for the high-risk group was not inferior to the other group, which suggested that age and leucocyte count influence outcomes only when HSCT could be performed during CR1. Based on the finding that the outcome of HSCT at non-remission was very poor (Tomizawa *et al*, 2009), we confirmed that intensified chemotherapy, which can achieve and maintain CR1 until HSCT, is essential in the treatment strategy for infants with high-risk ALL.

It is well recognized that recent progress in supportive therapy has resulted in a substantial reduction of the mortality rate (Gooley *et al*, 2010), and this was also reproduced in our cohort. Recent HCST was associated with a trend toward better outcomes in our cohort, although indication of HSCT did not differ during this study period.

TBI-based conditioning is the most potent and standard regimen for paediatric ALL (Davies *et al*, 2000; Bunin *et al*, 2003), but is associated with a higher incidence of late complications, especially in infants (Dvorak *et al*, 2011). Our results demonstrated that BU-based conditioning could be used as an alternative regimen and provided potentially better survival outcomes than TBI-based conditioning, with fewer late complications, such as secondary neoplasm (Curtis *et al*, 1997; Cohen *et al*, 2007; Schmiegelow *et al*, 2013). Although gonadal dysfunction is more problematic (Sarafoglou *et al*, 1997; Somali *et al*, 2005), the BU-based

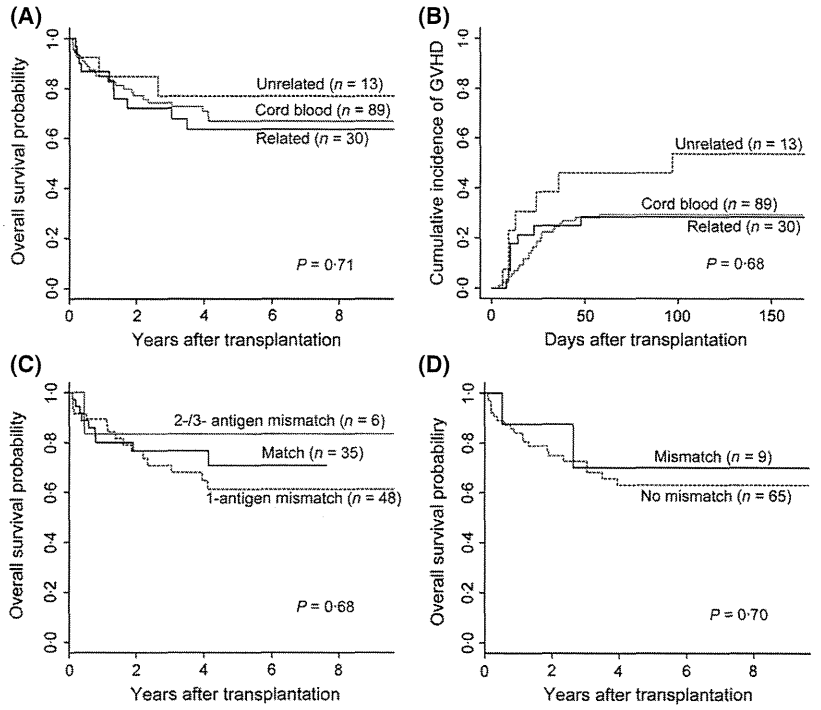

Fig 2. Stem cell sources and outcomes. (A) Overall survival according to stem cell source. (B) Cumulative incidence of grade II to IV acute graft-*versus*-host disease (GVHD). (C) Overall survival according to human leucocyte antigen (HLA) mismatches in cord blood transplantation. HLA disparities were defined as the number of serological mismatches. (D) Overall survival according to KIR ligand incompatibility.

Table III. Multivariate analysis of the risk factors for overall mortality (HSCT at CR1).

	Overall mortality	
Characteristic	Hazard ratio (95% CI)	*P*-value
Transplantation period		
1996–2003	1	0·07
2004–2011	0·40 (0·15–1·08)	
Age at transplantation (months)		
<3	1	0·93
3–5	1·05 (0·36–3·09)	
7–12	0·88 (0·28–2·80)	0·83
Initial leucocyte count ($\times 10^9$/l)		
<100	1	0·24
≥100	1·60 (0·73–3·50)	
Cytogenetics		
t(4;11)	1	0·25
Other *KMT2A*s	0·61 (0·26–1·43)	
Transplantation donor		
Related	1	0·73
Unrelated	1·32 (0·27–6·40)	
Cord blood	1·49 (0·51–4·37)	0·46
Transplantation conditioning		
Myeloablative BU	1	0·38
Myeloablative TBI	0·61 (0·20–1·86)	

95% CI, 95% confidence interval; BU, busulfan; TBI, total body irradiation.

regimen is assumed to be standard conditioning for infants with ALL.

In our cohort, CB was the main stem cell source, probably because of small body size of infants, and the types of stem cell sources and HLA disparities were not associated with survival. Previous studies reported that HLA mismatches could be a risk factor for paediatric leukaemia (Eapen *et al*, 2007); however, CB transplantation results in a large number of haematopoietic stem cells in infants due to their small body size, which could overcome the possible disadvantages associated with HLA disparities. The graft-*versus*-leukaemia (GVL) effect induced by a KIR ligand incompatibility could suppress the relapse of leukaemia (Willemze *et al*, 2009), and is more prominent in infants with ALL (Leung *et al*, 2004); however, we failed to confirm this finding in the present study.

This study retrospectively analysed registry data and naturally has some limitations. For example, data regarding late complications other than secondary malignancies, such as hormonal, pulmonary or neurocognitive dysfunction, is insufficient and inconsistencies were observed in the selection criteria for the stem cell source and conditioning regimen (BU or TBI), even though HSCT at CR1 had been principally indicated for infants with ALL during this period. Although this is one of the largest studies conducted on HSCT in infants with ALL, all of these subgroup analyses were underpowered due to the small sample size and wide confidence intervals, and the results obtained should be carefully interpreted. Therefore, further international studies in a large cohort are required to improve the treatment of infants with ALL with or without HSCT.

In conclusion, allogeneic HSCT with myeloablative BU conditioning is an important option for infants with high-risk ALL in CR1, and could provide similar survival probabilities regardless of the age at diagnosis, initial leucocyte count, *KMT2A* fusion partner of, and stem cell sources.

Acknowledgements

We would like to thank all the staff at the hospitals and centres that provided precise data via the registry of the Japan Society for Haematopoietic Cell Transplantation (JSHCT). A script kindly provided by Dr. Yoshinobu Kanda, Saitama Medical Centre, Jichi Medical University, was used for data manipulation. This work was supported in part by a Research Grant for Allergic Disease and Immunology from the Japanese Ministry of Health, Labor, and Welfare. All authors had no conflict of interest to disclose.

Author contributions

M.K is the principal investigator and takes primary responsibility for the paper. M.K, D.H. and K.Kato designed the research; K.Koh, K.Kato, J.T, J.I, H.Y, H.G, S.A, A.H, Y.T, A.S, and Y.A recruited the patients and collected the data. M.K analysed the data, and M.K, D.H, A.Yand K.Kato wrote the manuscript. All authors discussed the results and commented on the manuscript.

Supporting Information

Additional Supporting Information may be found in the online version of this article:

Figure S1. Overall survival probability in each subgroups.

References

Atsuta, Y., Suzuki, R., Yoshimi, A., Gondo, H., Tanaka, J., Hiraoka, A., Kato, K., Tabuchi, K., Tsuchida, M., Morishima, Y., Mitamura, M., Kawa, K., Kato, S., Nagamura, T., Takanashi, M. & Kodera, Y. (2007) Unification of hematopoietic stem cell transplantation registries in Japan and establishment of the TRUMP System. *International Journal of Hematology*, **86**, 269–274.

Bacigalupo, A., Ballen, K., Rizzo, D., Giralt, S., Lazarus, H., Ho, V., Apperley, J., Slavin, S., Pasquini, M., Sandmaier, B.M., Barrett, J., Blaise, D., Lowski, R. & Horowitz, M. (2009) Defining the intensity of conditioning regimens: working definitions. *Biology of Blood and Marrow Transplantation*, **15**, 1628–1633.

Bunin, N., Aplenc, R., Kamani, N., Shaw, K., Cnaan, A. & Simms, S. (2003) Randomized trial of busulfan vs total body irradiation containing conditioning regimens for children with acute lymphoblastic leukemia: a Pediatric Blood and Marrow Transplant Consortium study. *Bone Marrow Transplantation*, **32**, 543–548.

Cohen, A., Rovelli, A., Merlo, D.F., van Lint, M.T., Lanino, E., Bresters, D., Ceppi, M., Bocchini, V., Tichelli, A. & Socie, G. (2007) Risk for secondary thyroid carcinoma after hematopoietic stem-cell transplantation: an EBMT Late Effects Working Party Study. *Journal of Clinical Oncology*, **25**, 2449–2454.

Curtis, R.E., Rowlings, P.A., Deeg, H.J., Shriner, D.A., Socie, G., Travis, L.B., Horowitz, M.M., Witherspoon, R.P., Hoover, R.N., Sobocinski, K.A., Fraumeni, J.F. Jr & Boice, J.D. Jr (1997) Solid cancers after bone marrow transplantation. *New England Journal of Medicine*, **336**, 897–904.

Davies, S.M., Ramsay, N.K., Klein, J.P., Weisdorf, D.J., Bolwell, B., Cahn, J.Y., Camitta, B.M., Gale, R.P., Giralt, S., Heilmann, C., Henslee-Downey, P.J., Herzig, R.H., Hutchinson, R., Keating, A., Lazarus, H.M., Milone, G.A., Neudorf, S., Perez, W.S., Powles, R.L., Prentice, H.G., Schiller, G., Socie, G., Vowels, M., Wiley, J., Yeager, A. & Horowitz, M.M. (2000) Comparison of preparative regimens in transplants for children with acute lymphoblastic leukemia. *Journal of Clinical Oncology*, **18**, 340–347.

Dreyer, Z.E., Dinndorf, P.A., Camitta, B., Sather, H., La, M.K., Devidas, M., Hilden, J.M., Heerema, N.A., Sanders, J.E., McGlennen, R., Willman, C.L., Carroll, A.J., Behm, F., Smith, F.O., Woods, W.G., Godder, K. & Reaman, G.H. (2011) Analysis of the role of hematopoietic stem-cell transplantation in infants with acute lymphoblastic leukemia in first remission and MLL gene rearrangements: a report from the Children's Oncology Group. *Journal of Clinical Oncology*, **29**, 214–222.

Dvorak, C.C., Gracia, C.R., Sanders, J.E., Cheng, E.Y., Baker, K.S., Pulsipher, M.A. & Petryk, A. (2011) NCI, NHLBI/PBMTC first international conference on late effects after pediatric hematopoietic cell transplantation: endocrine challenges-thyroid dysfunction, growth impairment, bone health, & reproductive risks. *Biology of Blood and Marrow Transplantation*, **17**, 1725–1738.

Eapen, M., Rubinstein, P., Zhang, M.J., Stevens, C., Kurtzberg, J., Scaradavou, A., Loberiza, F.R., Champlin, R.E., Klein, J.P., Horowitz, M.M. & Wagner, J.E. (2007) Outcomes of transplantation of unrelated donor umbilical cord blood and bone marrow in children with acute leukaemia: a comparison study. *Lancet*, **369**, 1947–1954.

Gooley, T.A., Chien, J.W., Pergam, S.A., Hingorani, S., Sorror, M.L., Boeckh, M., Martin, P.J., Sandmaier, B.M., Marr, K.A., Appelbaum, F.R., Storb, R. & McDonald, G.B. (2010) Reduced mortality after allogeneic hematopoietic-cell transplantation. *New England Journal of Medicine*, **363**, 2091–2101.

Hilden, J.M., Dinndorf, P.A., Meerbaum, S.O., Sather, H., Villaluna, D., Heerema, N.A., McGlennen, R., Smith, F.O., Woods, W.G., Salzer, W.L., Johnstone, H.S., Dreyer, Z. & Reaman, G.H. & Children's Oncology, G. (2006) Analysis of prognostic factors of acute lymphoblastic leukemia in infants: report on CCG 1953 from the Children's Oncology Group. *Blood*, **108**, 441–451.

Inaba, H., Greaves, M. & Mullighan, C.G. (2013) Acute lymphoblastic leukaemia. *Lancet*, **381**, 1943–1955.

Jacobsohn, D.A., Hewlett, B., Morgan, E., Tse, W., Duerst, R.E. & Kletzel, M. (2005) Favorable outcome for infant acute lymphoblastic leukemia after hematopoietic stem cell transplantation. *Biology of Blood and Marrow Transplantation*, **11**, 999–1005.

Kosaka, Y., Koh, K., Kinukawa, N., Wakazono, Y., Isoyama, K., Oda, T., Hayashi, Y., Ohta, S., Moritake, H., Oda, M., Nagatoshi, Y., Kigasawa, H., Ishida, Y., Ohara, A., Hanada, R., Sako, M., Sato, T., Mizutani, S., Horibe, K. & Ishii, E. (2004) Infant acute lymphoblastic leukemia with MLL gene rearrangements: outcome following intensive chemotherapy and hematopoietic stem cell transplantation. *Blood*, **104**, 3527–3534.

Leung, W., Iyengar, R., Turner, V., Lang, P., Bader, P., Conn, P., Niethammer, D. & Handgretinger, R. (2004) Determinants of antileukemia effects of allogeneic NK cells. *Journal of Immunology*, **172**, 644–650.

Mann, G., Attarbaschi, A., Schrappe, M., De Lorenzo, P., Peters, C., Hann, I., De Rossi, G., Felice, M., Lausen, B., Leblanc, T., Szczepanski, T., Ferster, A., Janka-Schaub, G., Rubnitz, J., Silverman, L.B., Stary, J., Campbell, M., Li, C.K., Suppiah, R., Biondi, A., Vora, A., Valsecchi, M.G. & Pieters, R. & Interfant-99 Study, G. (2010) Improved outcome with hematopoietic stem cell transplantation in a poor prognostic subgroup of infants with mixed-lineage-leukemia (MLL)-rearranged acute lymphoblastic leukemia: results from the Interfant-99 Study. *Blood*, **116**, 2644–2650.

Nagayama, J., Tomizawa, D., Koh, K., Nagatoshi, Y., Hotta, N., Kishimoto, T., Takahashi, Y., Kuno, T., Sugita, K., Sato, T., Kato, K., Ogawa, A., Nakahata, T., Mizutani, S., Horibe, K.,Ishii, E. & Japan Infant Leukemia Study, G. (2006)

Infants with acute lymphoblastic leukemia and a germline MLL gene are highly curable with use of chemotherapy alone: results from the Japan Infant Leukemia Study Group. *Blood*, **107**, 4663–4665.

Pieters, R., Schrappe, M., De Lorenzo, P., Hann, I., De Rossi, G., Felice, M., Hovi, L., LeBlanc, T., Szczepanski, T., Ferster, A., Janka, G., Rubnitz, J., Silverman, L., Stary, J., Campbell, M., Li, C.K., Mann, G., Suppiah, R., Biondi, A., Vora, A. & Valsecchi, M.G. (2007) A treatment protocol for infants younger than 1 year with acute lymphoblastic leukaemia (Interfant-99): an observational study and a multicentre randomised trial. *Lancet*, **370**, 240–250.

Pui, C.H., Gaynon, P.S., Boyett, J.M., Chessells, J.M., Baruchel, A., Kamps, W., Silverman, L.B., Biondi, A., Harms, D.O., Vilmer, E., Schrappe, M. & Camitta, B. (2002) Outcome of treatment in childhood acute lymphoblastic leukaemia with rearrangements of the 11q23 chromosomal region. *Lancet*, **359**, 1909–1915.

Rubnitz, J.E., Camitta, B.M., Mahmoud, H., Raimondi, S.C., Carroll, A.J., Borowitz, M.J., Shuster, J.J., Link, M.P., Pullen, D.J., Downing, J.R., Behm, F.G. & Pui, C.H. (1999) Childhood acute lymphoblastic leukemia with the MLL-ENL fusion and t(11;19)(q23;p13.3) translocation. *Journal of Clinical Oncology*, **17**, 191–196.

Sanders, J.E., Im, H.J., Hoffmeister, P.A., Gooley, T.A., Woolfrey, A.E., Carpenter, P.A., Andrews, R.G., Bryant, E.M. & Appelbaum, F.R. (2005) Allogeneic hematopoietic cell transplantation for infants with acute lymphoblastic leukemia. *Blood*, **105**, 3749–3756.

Sarafoglou, K., Boulad, F., Gillio, A. & Sklar, C. (1997) Gonadal function after bone marrow transplantation for acute leukemia during childhood. *Journal of Pediatrics*, **130**, 210–216.

Schmiegelow, K., Levinsen, M.F., Attarbaschi, A., Baruchel, A., Devidas, M., Escherich, G., Gibson, B., Heydrich, C., Horibe, K., Ishida, Y., Liang, D.C., Locatelli, F., Michel, G., Pieters, R., Piette, C., Pui, C.H., Raimondi, S., Silverman, L., Stanulla, M., Stark, B., Winick, N. & Valsecchi, M.G. (2013) Second malignant neoplasms after treatment of childhood acute lymphoblastic leukemia. *Journal of Clinical Oncology*, **31**, 2469–2476.

Silverman, L.B., McLean, T.W., Gelber, R.D., Donnelly, M.J., Gilliland, D.G., Tarbell, N.J. & Sallan, S.E. (1997) Intensified therapy for infants with acute lymphoblastic leukemia: results from the Dana-Farber Cancer Institute Consortium. *Cancer*, **80**, 2285–2295.

Somali, M., Mpatakoias, V., Avramides, A., Sakellari, I., Kaloyannidis, P., Smias, C., Anagnostopoulos, A., Kourtis, A., Rousso, D., Panidis, D. & Vagenakis, A. (2005) Function of the hypothalamic-pituitary-gonadal axis in long-term survivors of hematopoietic stem cell transplantation for hematological diseases. *Gynecological Endocrinology*, **21**, 18–26.

Tomizawa, D., Koh, K., Sato, T., Kinukawa, N., Morimoto, A., Isoyama, K., Kosaka, Y., Oda, T., Oda, M., Hayashi, Y., Eguchi, M., Horibe, K., Nakahata, T., Mizutani, S. & Ishii, E. (2007) Outcome of risk-based therapy for infant acute lymphoblastic leukemia with or without an MLL gene rearrangement, with emphasis on late effects: a final report of two consecutive studies, MLL96 and MLL98, of the Japan Infant Leukemia Study Group. *Leukemia*, **21**, 2258–2263.

Tomizawa, D., Koh, K., Hirayama, M., Miyamura, T., Hatanaka, M., Saikawa, Y. & Ishii, E. (2009) Outcome of recurrent or refractory acute lymphoblastic leukemia in infants with MLL gene rearrangements: a report from the Japan Infant Leukemia Study Group. *Pediatric Blood & Cancer*, **52**, 808–813.

Willemze, R., Rodrigues, C.A., Labopin, M., Sanz, G., Michel, G., Socie, G., Rio, B., Sirvent, A., Renaud, M., Madero, L., Mohty, M., Ferra, C., Garnier, F., Loiseau, P., Garcia, J., Lecchi, L., Kogler, G., Beguin, Y., Navarrete, C., Devos, T., Ionescu, I., Boudjedir, K., Herr, A.L., Gluckman, E., Rocha, V. & Eurocord, N. & Acute Leukaemia Working Party of the, E. (2009) KIR-ligand incompatibility in the graft-versus-host direction improves outcomes after umbilical cord blood transplantation for acute leukemia. *Leukemia*, **23**, 492–500.

Published OnlineFirst March 27, 2014; DOI: 10.1158/0008-5472.CAN-13-2470

Molecular and Cellular Pathobiology

Cancer Research

Biallelic *DICER1* Mutations in Sporadic Pleuropulmonary Blastoma

Masafumi Seki[1], Kenichi Yoshida[2,6], Yuichi Shiraishi[3], Teppei Shimamura[3], Yusuke Sato[2,6], Riki Nishimura[1], Yusuke Okuno[2], Kenichi Chiba[3], Hiroko Tanaka[4], Keisuke Kato[7], Motohiro Kato[1,5,8], Ryoji Hanada[5], Yuko Nomura[9], Myoung-Ja Park[10], Toshiaki Ishida[11], Akira Oka[1], Takashi Igarashi[1,12], Satoru Miyano[3,4], Yasuhide Hayashi[9], Seishi Ogawa[2,6], and Junko Takita[1]

Abstract

Pleuropulmonary blastoma (PPB) is a rare pediatric malignancy whose pathogens are poorly understood. Recent reports suggest that germline mutations in the microRNA-processing enzyme DICER1 may contribute to PPB development. To investigate the genetic basis of this cancer, we performed whole-exome sequencing or targeted deep sequencing of multiple cases of PPB. We found biallelic *DICER1* mutations to be very common, more common than *TP53* mutations also found in many tumors. Somatic ribonuclease III (RNase IIIb) domain mutations were identified in all evaluable cases, either in the presence or absence of nonsense/frameshift mutations. Most cases had mutated *DICER1* alleles in the germline with or without an additional somatic mutation in the remaining allele, whereas other cases displayed somatic mutations exclusively where the RNase IIIb domain was invariably affected. Our results highlight the role of RNase IIIb domain mutations in *DICER1* along with TP53 inactivation in PPB pathogenesis. *Cancer Res; 74(10); 2742–9. ©2014 AACR.*

Introduction

Pleuropulmonary blastoma (PPB) is an extremely rare and highly aggressive pulmonary malignancy occurring in early childhood. It is characterized histologically by a primitive blastoma and a malignant mesenchymal stroma in the lung that often shows multidirectional differentiation (1). PPB may be sporadic or hereditary and may also present as a part of a familial tumor syndrome (2) consisting of cystic nephroma and other tumor types, such as ovarian tumor, embryonal rhabdomyosarcoma, and malignant germ cell tumors (2). Recently, germline *DICER1* mutations have been demonstrated in majority of patients with PPB and DICER1 syndrome (2, 3). *DICER1* is a member of the ribonuclease III (RNase III) protein family that is involved in the generation of microRNAs (miRNA), modulating gene expression at the posttranscriptional level (4). The DICER1 protein contains RNase IIIa and RNase IIIb domains, which are considered to dimerize intramolecularly with Mg^{2+}/Mn^{2+} to form the active site of the enzyme (5). In PPB, almost all mutations are reported to be heterozygous frameshift or nonsense mutations of germline origin, suggesting an important role of *DICER1* haploinsufficiency in PPB pathogenesis (2, 3). However, most obligate carriers of *DICER1* mutations and heterozygous *Dicer1*-deficient mice did not develop PPB or other types of tumors, suggesting that *DICER1* haploinsufficiency alone is insufficient for tumor development but requires additional genetic alterations (3, 6). To identify a complete set of genetic alterations underlying PPB pathogenesis, we performed whole-exome sequencing of paired tumor and normal DNA from seven cases with sporadic PPB, of which two cases were analyzed for samples obtained at both initial presentation and relapse. Mutations in *DICER1* and other genes were examined by targeted deep sequencing in 16 samples from 12 sporadic PPB cases, including three analyzed by whole-exome sequencing.

Materials and Methods

Specimens

Genomic DNA for 11 cases was extracted from fresh-frozen samples stored at −80 °C and obtained approximately 2 to 15 years previously. Paraffin-embedded samples were used as tumor samples for cases 10 (at relapse) and 11 (at diagnosis). These samples were stored for approximately 1 year. For

Authors' Affiliations: [1]Department of Pediatrics; [2]Cancer Genomics Project, Graduate School of Medicine; Laboratory of [3]DNA Information Analysis and [4]Sequence Data Analysis, Human Genome Center, Institute of Medical Science; [5]Department of Cell Therapy and Transplantation Medicine, The University of Tokyo, Tokyo; [6]Department of Pathology and Tumor Biology, Graduate School of Medicine, Kyoto University, Kyoto; [7]Division of Pediatric Hematology and Oncology, Ibaraki Children's Hospital, Mito, Ibaraki; [8]Department of Hematology/Oncology, Saitama Children's Medical Center, Saitama, Saitama; [9]Department of Pediatrics, School of Medicine, Fukuoka University, Fukuoka; [10]Gunma Children's Medical Center, Shibukawa, Gunma; [11]Department of Hematology and Oncology, Hyogo Prefectural Kobe Children's Hospital, Kobe, Hyogo; and [12]National Center for Child Health and Development, Tokyo, Japan

Note: Supplementary data for this article are available at Cancer Research Online (http://cancerres.aacrjournals.org/).

Corresponding Authors: Junko Takita, Department of Pediatrics, The University of Tokyo, 7-3-1 Hongo, Bunkyo-ku, Tokyo 113-8655, Japan. Phone: 81-3-3815-5411; Fax: 81-3-3816-4108; E-mail: jtakita-tky@umin.ac.jp; and Seishi Ogawa, Department of Pathology and Tumor Biology, Graduate School of Medicine, Kyoto University, Yoshida-Konoe-cho, Sakyo-ku, Kyoto 606-8501, Japan. Phone: 81-75-753-4300; Fax: 81-75-753-9282; E-mail: sogawa-tky@umin.ac.jp

doi: 10.1158/0008-5472.CAN-13-2470

Published OnlineFirst March 27, 2014; DOI: 10.1158/0008-5472.CAN-13-2470

germline control, DNA was obtained from bone marrow blood, peripheral blood, or bone marrow smears in which absence of tumor cells was pathologically confirmed. Bone marrow smears were used as normal samples for cases 05, 07, 08, and 12. This study was approved by The University of Tokyo Ethics Committee (Tokyo, Japan; approval number 1598), and informed consent was obtained from the parents of all participants.

Whole-exome sequencing

Whole-exome sequencing of primary tumor and matched normal specimens of cases 01, 02, 04, 07, 09, 10, and 12 was performed as previously described (7, 8). Relapsed tumor specimens of cases 01 and 02 were also analyzed. Whole-exome capture was accomplished using liquid-phase hybridization of sonicated genomic DNA having a 150 to 200-bp mean length to a bait cRNA library synthesized on magnetic beads (SureSelect Human All Exon Kit V3 or V5, Agilent Technology) according to the manufacturer's protocol. The captured targets were subjected to sequencing using HiSeq 2000 (Illumina) according to the manufacturer's instructions. Raw sequence data were processed using Genomon-exome (http://genomon.hgc.jp/exome/en/index.html) for detection of cancer exome sequencing data through the in-house pipeline constructed at the Human Genome Center, the Institute of Medical Science, The University of Tokyo. Analyses using Genomon are summarized in Supplementary Fig. S1. Sequence data have been deposited at the European Genome-phenome Archive (EGA, http://www.ebi.ac.uk/ega/), which is hosted by the European Bioinformatics Institute, under accession number EGAS00001000662.

Deep sequencing for validation of variants detected by whole-exome sequencing

To validate the mutations detected by whole-exome sequencing, deep sequencing was performed using pair or trio DNA specimens (primary/relapse tumor and normal) using HiSeq 2000 or MiSeq (Illumina). Primers used for this validation are listed in Supplementary Table S1. Mutations were amplified using PCR with a *Not*I linker individually attached to each primer and pooled together on a per-sample basis after successful amplification was confirmed by gel electrophoresis. Pooling was followed by purification of DNA using the FastGene Gel/PCR Extraction Kit (Nippon Genetics) and digestion with *Not*I. The digested DNA was purified again, and an aliquot of purified DNA was ligated with T4 DNA ligase for 5 hours, sonicated into approximately 200 bp fragments on an average using Covaris (Covaris), and used for generation of sequencing libraries with the NEBNext Ultra DNA Library Prep Kit for Illumina (New England Biolabs) according to the manufacturer's protocol. Data processing was performed according to previously described methods (7, 8). Each single-nucleotide variant and each insertion/deletion (indel) whose variant allele frequency (VAF) in the tumor sample was equal to or more than 2.0% and in the germline sample less than 2.0% were assigned as a somatic mutation. If the mutant allele frequency in the matched nontumor sample was more than 2.0%, the mutation was discarded (8). The mutation was evaluated for pathogenicity using the online mutation predicting tool, Mutation Taster (http://www.mutationtaster.org).

Small RNA sequencing

RNA was extracted using the miRNeasy Kit (Qiagen). Total RNA was quantified and evaluated for quality using a bioanalyzer (Agilent Technology). Libraries for small RNA sequencing were generated using the TruSeq small RNA Sample Preparation Kit (Illumina) and analyzed using the Illumina MiSeq according to the manufacturer's protocol. Small RNA sequencing was performed for four cases (cases 01, 07, 08, and 09). Read sequences were aligned against miRBase (release 16) using MiSeq Reporter v2.3 (Illumina). After alignment, the number of read sequences aligned to each miRNA or pre-miRNA was calculated. Gurtan and colleagues demonstrated that the RNase IIIA and IIIB domains of DICER1 process the 3′ (3p) and 5′ (5p) arms of miRNAs, respectively, *in vivo* (9). We defined the pre-miRNA cleavage ratio as the read counts of miRNA/(read counts of pre-miRNA + miRNA). This ratio was calculated for 5p or 3p miRNA, and then compared tumor specimens with fetal lung as normal control. Statistical differences were calculated by Wilcoxon rank-sum test.

Single-nucleotide polymorphism genotyping microarray

DNA of 11 cases (excluding case 11) as well as that of three relapse cases was hybridized to Affymetrix GeneChip 250K Nsp arrays (Affymetrix). DNA of cases 10 (at relapse) and 11 was not hybridized because of the poor quality of DNA from the paraffin-embedded samples. After appropriate normalization of mean array intensities, signal ratios between tumors and anonymous normal references were calculated in an allele-specific manner, and allele-specific copy numbers were inferred from the observed signal ratios based on a hidden Markov model using CNAG software (http://www.genome.umin.jp).

Sanger sequencing and targeted deep amplicon sequencing

Sanger sequencing of *DICER1* and *TP53* was performed for samples from all cases and relapsed tumor samples from four cases. Germline DNA was sequenced for nine cases (including case 02 without *DICER1* mutation). Sanger sequencing of *PDCD2L* and *UBA2* was performed for 11 cases. Deep amplicon sequencing of target exons of *TP53*, *GPR182*, and *CTNNB1* was performed for 14 samples from 11 cases. Exons harboring mutations in *DICER1* were sequenced for 11 cases, and all coding exons of *DICER1* were sequenced for case 02. Details of deep sequencing have been provided above. All primer sequences for these genes are listed in Supplementary Table S2–S4.

Results

The mean coverage in the whole-exome sequencing of tumor and germline samples was 126× and 128× for the 50 Mb target regions, respectively. More than 93% of the coding sequences were represented by more than 20 independent reads on an average (Supplementary Fig. S2). GC content and mean coverage are shown in Supplementary Fig. S3. Mean coverage of high-GC (≥60%) exons was lower than that of low GC (<60%). In total, 217 nonsilent substitutions and 12 indels

Published OnlineFirst March 27, 2014; DOI: 10.1158/0008-5472.CAN-13-2470

were detected across nine tumor specimens, of which 191 (88%) and 12 (100%), respectively, were successfully confirmed by deep sequencing (Supplementary Table S5). The number of nonsilent mutations per sample at presentation (13–35 mutations) was lower than that reported in most solid tumors in adults (10–12), but comparable with the number reported for other pediatric tumors such as neuroblastoma and medulloblastoma (18 and 16, respectively; Fig. 1A; refs. 13, 14). In two cases for which serial samples could be analyzed, relapsed samples had higher mutation number than corresponding samples at initial presentation (Fig. 1A and B). In both cases, intratumoral subpopulations were evident at the time of initial presentation (Fig. 1C). As previously reported for other cancers (15, 16), the clonal architecture of tumor subpopulations underwent dynamic evolutionary alterations during tumor progression. Serial samples in each case had several clonal mutations in common as well as harbored private subclonal mutations of their own (Fig. 1B and C). In case 01, some of the subclonal mutations (purple) found in the initial sample disappeared at relapse and were replaced by new mutations carried by new subpopulations (red), whereas most of the mutations found in the subclones (green) were retained at similar relative allele frequencies in the relapse sample in case 02. In both cases, relapsed tumors were accompanied by newly acquired gene mutations in each subpopulation and/or by appearance of new subclones that were totally absent from the original initial samples (Fig. 1C).

DICER1 mutations were detected for six cases (cases 01, 04, 07, 09, 10, and 12) but not for case 02; targeted deep sequencing was unable to detect any *DICER1* mutations. *DICER1* mutations were found in the major tumor populations in these six cases (Fig. 1C and D). In contrast with previous reports where all *DICER1* mutations were heterozygous and had germline origin, we identified two homozygous somatic *DICER1* mutations in cases 09 and 10, prompting us to investigate the status of *DICER1* mutations in five additional cases. *DICER1* mutations were found in 11 of 12 (92%) cases (Table 1; Fig. 2A and Supplementary Fig. S4), in which six of the 11 cases with *DICER1* mutations carried compound heterozygous mutations. Two cases carried homozygous *DICER1* mutations (Fig. 2B), presumably caused by copy number-neutral LOH (or uniparental disomy; UPD) involving the 14q arm harboring the *DICER1* locus. In total, biallelic *DICER1* mutations were found in eight of the 11 (73%) cases with *DICER1* mutations. We failed to demonstrate biallelic alterations in three cases (case 01, 05, and 11; Table 1 and Supplementary Fig. S4). We confirmed the same *DICER1* mutation status in initial and relapse samples in all four cases, for which both serial samples were available, indicating that *DICER1* mutations are involved in tumor development rather than progression.

Germline DNA was available in eight cases to confirm germline/somatic origins of *DICER1* mutations, of which four (cases 04, 07, 08, and 12) were compound heterozygous for a germline nonsense/frameshift and a somatic missense mutation, two (cases 09 and 10) were homozygous for somatic, missense mutations caused by an acquired UPD, and the remaining cases were heterozygous for a somatic missense mutation (case 01) or a germline frameshift mutation (case 05;

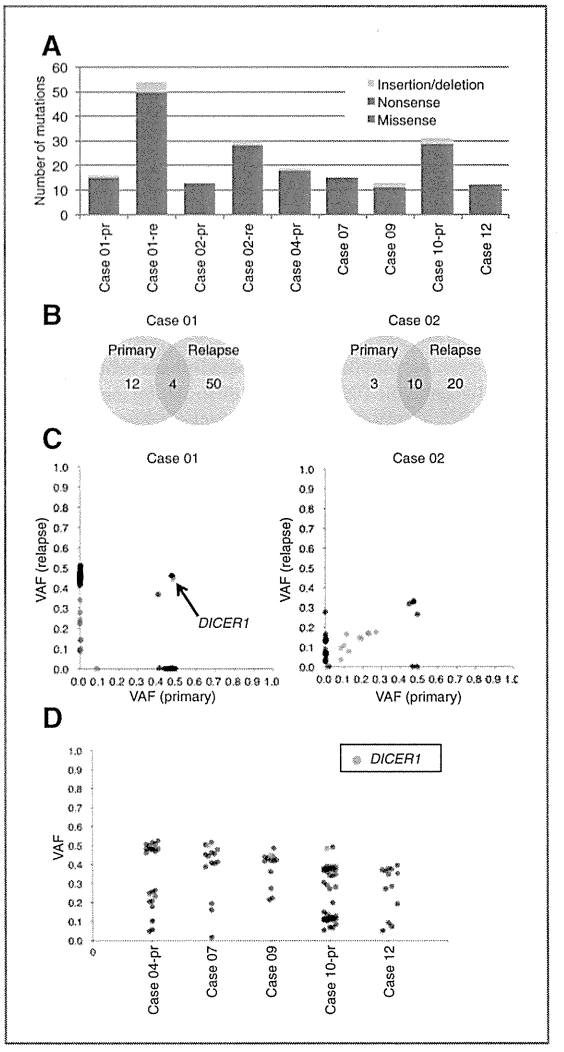

Figure 1. Mutations and mutant allele frequencies detected by whole-exome sequencing in 7 PPB cases. A, type and number of somatic mutations in each tumor. Each mutation type is distinguished using the indicated color. Primary (pr) and relapsed (re) tumors of cases 01 and 02 were examined independently by whole-exome sequencing. B, Venn diagram of somatic mutations found in cases 01 and 02. Both relapsed (re) tumors had increased number of somatic mutations compared with primary (pr) tumors. C, VAF distribution of validated mutations in relapsed cases. VAF was obtained from deep sequencing. Allele frequencies were corrected for copy numbers determined by SNP array analysis. *DICER1* mutation is discriminated by the indicated color in case 01. Case 02 harbored no *DICER1* mutation. Subclonal mutations in case 01 at primary (pr) and relapse (re) are distinguished by purple and red, respectively. Subclonal mutations in case 02 are distinguished by green. D, VAF distribution of validated mutations in nonrelapsed cases. *DICER1* mutations were included in the major tumor population.

Table 1). Among the three cases without normal samples, the combination of a nonsense and missense mutation was also found in the two cases with compound heterozygous mutations. In these cases, a somatic origin was suspected for a

Published OnlineFirst March 27, 2014; DOI: 10.1158/0008-5472.CAN-13-2470

Table 1. Mutations in *DICER1* and *TP53* in sporadic PPB cases

	DICER1				*TP53*				
Case	**Exon**	**Mutation**	**AA change**	**Origin**	**Exon**	**Mutation**	**AA change**	**17p**	**Sample**
01	25	5428G>T	D1810Y	Somatic		Native		Loss	Pr/Re
02		Native				Native			Pr/Re
03	23	4910C>A	S1637X	ND	4	c.332_333delTG	p.L111fs	Loss	Pr
	24	5114A>T	E1705V	ND					
04	21	3482delC	P1161fs	Germline	5	c.527G>T[a]	p.C176F	Loss	Pr/Re
	24	5125G>A	D1709N	Somatic	4	c.313G>A[b]	p.G105S		
05	9	1383delAAAG	I461fs	Germline		Native			Pr
06	19	3007C>T	R1003X	ND		Native			Pr
	25	5428G>T	D1810Y	Probably somatic					
07	18	2863insA	T955fs	Germline	8	c.891_903	p.H297fs	Loss	Pr
	25	5425G>A	G1809R	Somatic		delCGAGCTGCCCCCA			
08	21	3748delC	S1250fs	Germline	7	c.762_764delACAT	p.I254fs	Loss	Pr
	25	5425G>A	G1809R	Somatic					
09	25	5425G>A (Homozygous)	G1809R	Somatic		Native		Loss	Pr
10	25	5425G>A (Homozygous)	G1809R	Somatic	8	c.817C>T	p.R273C	Loss	Pr/Re
11	8	1148dupAGGGT	I383fs	ND		Native		ND	Pr
12	25	5460C>G	Y1820X	Germline		Native		Loss	Pr
	25	5438A>G	E1813G	Somatic					

Abbreviations: ND, not determined; AA, amino acid; Pr, primary; Re, relapse.
[a]Primary tumor.
[b]Relapse tumor.

missense mutation (D1810Y) in case 06, in that the VAF of that mutant deviated significantly from the expected value (0.5) for germline variants (Supplementary Table S6). Conspicuously, all the nine missense *DICER1* mutations found in our cohort were located within the RNase IIIb domain with a mutational hotspot at G1809 (Fig. 2C), for which a somatic origin was confirmed or highly suspected in eight mutations. Combined with previous reports for PPB (2, 3), this high frequency of germline mutations supported the incomplete penetrance of *DICER1* mutations in both familial and sporadic PPB. To assess the effect of *DICER1* mutation in RNase IIIb domain on RNA cleavage, we performed small RNA sequencing in tumors with mutational hotspots at G1809R and D1810Y. Total RNA including miRNA extracted from fetal lung was used as a normal control. Given that the RNase IIIA and IIIB domains of DICER1 process the 3p and 5p arms of miRNAs, respectively (9), *DICER1* mutations in RNase IIIb domain are expected to affect 5p rather than 3p miRNA expression. Comparing the pre-miRNA cleavage ratio of tumor samples to that of the fetal lung control, we confirmed dramatically reduced 5p miRNA expression in the tumors with G1809R and D1810Y mutations ($P < 7.1 \times 10^{-7}$; Fig. 3A and B). In contrast, 3p miRNA expression was significantly higher in the tumor samples than in fetal lung control ($P < 1.4 \times 10^{-3}$), suggesting that G1809R and D1810Y mutants have opposite effects on 3p miRNA cleavage. Taken together, our results suggest that a mutational hotspot at G1809R has a pathogenic effect.

Except for *DICER1*, several genes were found to be recurrently mutated in whole-exome sequencing, including *TP53*, *CTNNB1*, *GPR182*, *MYH8*, *PDE2A*, and *TMX3* (Supplementary Table S7). *TP53*, *CTNNB1*, and *GPR182* were investigated by targeted deep sequencing in an additional five cases, although these genes were not mutated in *CTNNB1* and *GPR182*. The result of targeted deep sequencing in *TP53* is described below. To identify additional genetic alterations, we next performed single-nucleotide polymorphism (SNP) array-based genome-wide copy number analysis in 14 samples of 11 cases for which high-quality genomic DNA was available (including three cases with both primary and relapsed tumors). Chromosome 8q gain was the most common copy number change and was found in 10 of the 11 cases in varying combinations with other genetic changes, including loss of chromosomes 10 and 17p and high-grade amplification of 19q (Fig. 4A and Supplementary Figs. S4 and S5). Chromosome 17p LOH was found in 10 samples and was caused by UPD ($N = 1$) or deletions ($N = 9$), and commonly involved an 8.5-Mb region that contained *TP53*. To investigate a possible role of *TP53* mutations in PPB, we analyzed the *TP53* mutation status in 14 tumor samples from all 12 cases by Sanger and deep sequencing. We detected recurrent missense or frame shift mutations in five of the 12 cases (42%; Fig. 4B; Table 1), in which all five cases were accompanied by 17p LOH and led to biallelic *TP53* inactivation. Intriguingly, in case 04, the relapsed tumor had a different *TP53* mutation (G105S) from that found at the time of initial presentation (C176F), suggesting that the relapse originated from a different subclone in which the two *DICER1* mutations predated *TP53* mutations. We also found several focal amplifications involving 5q23, 6q16-21, 15q23-24, and 19q13.11. However, none of

Published OnlineFirst March 27, 2014; DOI: 10.1158/0008-5472.CAN-13-2470

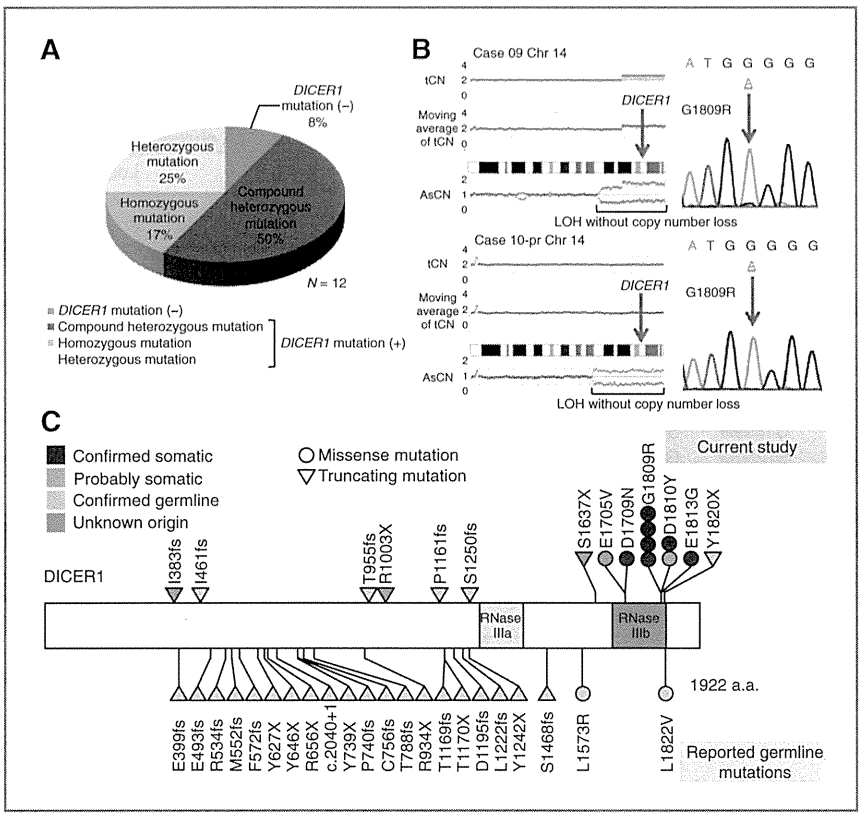

Figure 2. DICER1 abnormalities detected in 12 PPB cases. A, frequency of identified *DICER1* mutations in 12 cases. B, homozygous *DICER1* mutation with 14q LOH without copy number loss. Right panels show a sequence chromatogram of a G1809R homozygous mutation. Left panels show 14q LOH obtained from SNP array analysis. tCN, total copy number; AsCN, allele-specific copy number. C, a schematic of DICER1 protein structure with the positions of alterations. Top and bottom portions indicate mutations detected in our study and previously reported mutations in references 2 and 3, respectively. All the nine missense *DICER1* mutations found in our cohort were located within the RNase IIIb domain with a mutational hotspot at G1809. fs, frameshift.

these amplifications were recurrent, except for those involving 19q13.11, which were found in three (25%) of the 12 cases (Supplementary Fig. S5). The amplified region contains five genes, including *LSM14A*, *KIAA0355*, *GPI*, *UBA2*, and *PDCD2L*, but mutations were detected in none of these genes.

Discussion

The most striking discovery in the present study is the frequent biallelic involvement of *DICER1* mutations in majority of PPB cases with an obligatory missense mutation involving the RNase IIIb domain. In our cohort, biallelic *DICER1* mutations were documented in eight of the 11 *DICER1*-mutated cases with sporadic PBB, with RNase IIIb domain-involving mutations found in all cases and somatic origins demonstrated in all evaluable cases. This result was in stark contrast with previous reports, where all *DICER1* mutations in PPB or *DICER1* syndrome cases were heterozygous and inherited from parents; all mutations were either nonsense or frameshift changes except for two cases, of which one had a missense mutation in the RNase III domain (2, 3). Interestingly, a recent study reported frequent recurrent *DICER1* mutations affecting the RNase IIIb domain in nonepithelial ovarian cancers, especially Sertoli–Leydig cell tumor, in which 26 of 43 tumors carried exclusively RNase IIIb domain mutations with only four tumors being compound heterozygotes of a germline nonsense/frameshift mutation and an RNase IIIb domain mutation (5). Conspicuously, no germline mutations involving the RNase IIIb domain and no biallelic nonsense or frameshift mutations have been reported in any human cancers, possibly accounting for the different spectrum of *DICER1* mutations between PPB and ovarian cancers. These unique features of *DICER1* mutations suggest distinct oncogenic roles of both nonsense/frameshift and RNase IIIb domain mutations. It could be hypothesized that complete loss of DICER1 functions caused by biallelic nonsense/frameshift mutations is not compatible with cell viability, whereas further loss of particular DICER function, beyond haploinsufficiency through targeted mutations within the RNase IIIb domain, could be required or effective for the tumor cells to be clonally selected.

The RNase IIIb domain in DICER1 and other RNase III protein family members is involved in excision of double-stranded miRNA stems, which are then cleaved to single-stranded miRNA through the activity of the RNase IIIa domain (5). A mutation of the conserved amino acids in the RNase IIIb domain could thus lead to compromised miRNA processing, especially in excision of miRNAs. In fact, four mutational hotspots at metal-binding sites (E1705, D1709, D1810, and E1813) found in nonepithelial ovarian cancer were shown to have decreased RNase IIIb activity (5). In the current study, we found an additional mutational hotspot within the RNase IIIb domain affecting a highly conserved amino acid position

Published OnlineFirst March 27, 2014; DOI: 10.1158/0008-5472.CAN-13-2470

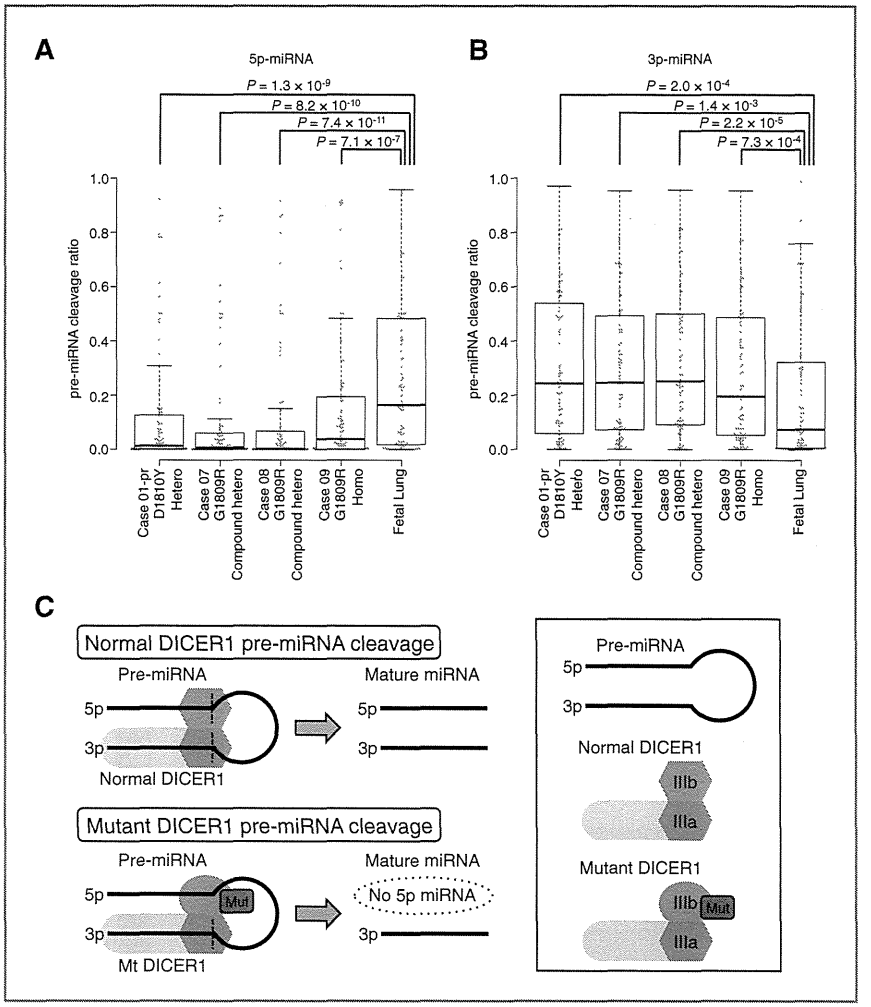

Figure 3. Significant reduction of pre-miRNA cleavage of 5p strand in four tumor specimens by small RNA sequencing. A, 5p miRNA biogenesis was significantly reduced in tumor samples. *P* values were calculated by Wilcoxon rank-sum test. B, 3p miRNA biogenesis was retained in tumor samples. In contrast with 5p miRNA expression, 3p miRNA expression in tumor samples exceeds normal control. C, schematic model of aberrant pre-miRNA cleavage by hotspot mutant DICER1. The miRNA biogenesis pathway by normal DICER1 is indicated in the top panel. A proposed model of hotspot DICER1 mutant is presented in the lower panel. Hotspot DICER1 mutant could not cleave the 5p strand of pre-miRNA. Loss of 5p miRNA may prompt DICER1 to cleave pre-miRNA so that 3p miRNA may be overprocessed.

(G1809) in the vicinity of the two known hotspot codons (D1810 and E1813). Our small RNA sequencing revealed that mutational hotspots at G1809 and a D1810 mutation showed a dramatically reduced cleavage ratio of 5p miRNA, and D1810 mutation also showed the same results in PPB. D1810 mutation is one of the hotspot mutations in nonepithelial ovarian cancer (5), of which reduced 5p miRNA expression has been already confirmed (17). This finding suggests that a specific mutational hotspot of PPB, G1809, is functionally equivalent to hotspot mutations in nonepithelial ovarian cancer. Anglesio and colleagues showed no significant change in 3p miRNA expression (17); however, its cleavage ratio was increased in our analysis. This result may be due to the existence of some mechanism that activates DICER1 to compensate the loss of 5p miRNA production (Fig. 3C). Gurtan and colleagues also mentioned an increased ratio of miRNA star to mature strands relative to cells expressing native hsDicer (9). MiRNA star means less abundant mature miRNA, which usually consists of 3p miRNA, so that this result is compatible with our observation. Thus, it seems that mutations at G1809 could lead to a biologic consequence similar to that of known hotspot mutations (5), although the oncogenic mechanism of the defective cleavage but not excision of miRNAs in the pathogenesis of PPB and other cancers awaits elucidation.

Besides *DICER1* mutations, *TP53* mutations with or without 17p loss as well as trisomy 8 and other chromosomal abnormalities were among the common genetic lesions in PPB. With respect to *DICER1* mutations, it is of note that TP53 also plays a critical role in the regulation of miRNA processing (18). Indeed, tumor-derived transcriptionally inactive TP53 mutants suppress precursor and mature miRNA levels, whereas native TP53 increases them (18), indicating that *TP53* plays an important role in cancer biology via regulation of miRNA processing. A recent study showed that TP53 regulates DICER1 expression via transcriptional miRNAs such as let-7 (19). In contrast, Wang and colleagues showed that knockdown of *DICER1*

Published OnlineFirst March 27, 2014; DOI: 10.1158/0008-5472.CAN-13-2470

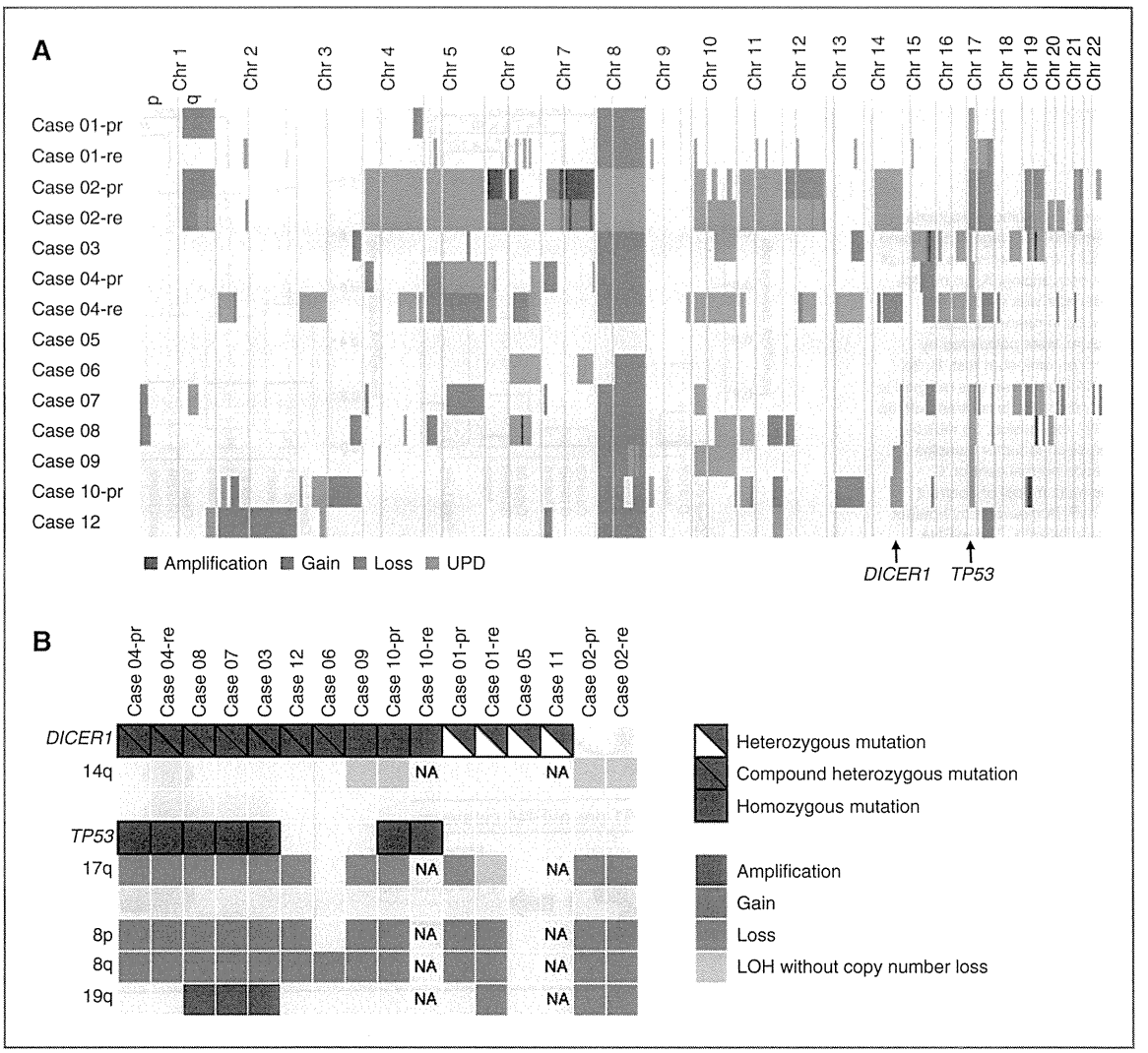

Figure 4. Overview of *DICER1* and *TP53* mutations with copy number alterations. A, copy number alterations by SNP array analysis in 14 PPB samples from 11 cases. The regions of *DICER1* and *TP53* are indicated by arrows. Amplification, gain, loss, and UPD are distinguished by the indicated colors. Copy number (CN) gain was defined as copy number between 3 and 5. Amplification was defined as an inferred copy number of more than 5. Copy number loss was defined as copy number less than one copy and LOH was assigned when one allele was retained. B, distribution of *DICER1* and *TP53* mutations with frequently detected copy number alterations. pr, primary; re, relapse; NA, not available.

expression in BxPC-3 and Panc-1 pancreatic cancer cells resulted in significant increases in TP53 protein levels (20), suggesting the existence of a regulatory loop between TP53, DICER1, and let-7, deregulation of which may play a role in PPB development.

In conclusion, biallelic *DICER1* mutations were common in PPB, invariably accompanied by a somatic RNase IIIb domain mutation. Majority of cases had mutated *DICER1* alleles in germline with or without an additional RNase IIIb domain mutation in the remaining allele. Recurrent mutations were rare in PPB, except for frequent *TP53* deletions/mutations. Our results provide novel insight into the critical role of *DICER1* mutations and importance of *TP53* inactivation in the pathogenesis of PPB.

Disclosure of Potential Conflicts of Interest

No potential conflicts of interest were disclosed.

Authors' Contributions

Conception and design: M. Seki, S. Ogawa, J. Takita
Development of methodology: Y. Shiraishi, Y. Okuno
Acquisition of data (provided animals, acquired and managed patients, provided facilities, etc.): M. Seki, K. Yoshida, Y. Sato, R. Nishimura, Y. Okuno, K. Kato, R. Hanada, Y. Nomura, M.-J. Park, T. Ishida

Published OnlineFirst March 27, 2014; DOI: 10.1158/0008-5472.CAN-13-2470

Analysis and interpretation of data (e.g., statistical analysis, biostatistics, computational analysis): M. Seki, Y. Shiraishi, T. Shimamura, Y. Sato, Y. Okuno, K. Chiba, H. Tanaka, S. Miyano
Writing, review, and/or revision of the manuscript: M. Seki, A. Oka, S. Ogawa, J. Takita
Administrative, technical, or material support (i.e., reporting or organizing data, constructing databases): T. Ishida, Y. Hayashi
Study supervision: T. Igarashi, Y. Hayashi, S. Ogawa, J. Takita

Acknowledgments

The authors thank Matsumura, Hoshino, Yin, Saito, Mori, Nakamura, Mizota, and Drs. K. Ohki and J. Okubo for excellent technical assistance and Drs. Y. Tanaka, K. Ida, A. Motomura, R. Shiozawa, K. Watanabe, and A. Kozaki for assisting with clinical care for patients and collecting samples.

References

1. Hill DA, Jarzembowski JA, Priest JR, Williams G, Schoettler P, Dehner LP. Type I pleuropulmonary blastoma: pathology and biology study of 51 cases from the international pleuropulmonary blastoma registry. Am J Surg Pathol 2008;32:282–95.
2. Hill DA, Ivanovich J, Priest JR, Gurnett Ca, Dehner LP, Desruisseau D, et al. DICER1 mutations in familial pleuropulmonary blastoma. Science 2009;325:965.
3. Slade I, Bacchelli C, Davies H, Murray a, Abbaszadeh F, Hanks S, et al. DICER1 syndrome: clarifying the diagnosis, clinical features and management implications of a pleiotropic tumour predisposition syndrome. Am J Med Genet 2011;48:273–8.
4. Carthew RW. Gene regulation by microRNAs. Curr Opin Genet Dev 2006;16:203–8.
5. Heravi-Moussavi A, Anglesio MS, Cheng SW, Senz J, Yang W, Prentice L, et al. Recurrent somatic DICER1 mutations in nonepithelial ovarian cancers. N Engl J Med 2012;366:234–42.
6. Kumar MS, Pester RE, Chen CY, Lane K, Chin C, Lu J, et al. Dicer1 functions as a haploinsufficient tumor suppressor. Genes Dev 2009;23:2700–4.
7. Yoshida K, Sanada M, Shiraishi Y, Nowak D, Nagata Y, Yamamoto R, et al. Frequent pathway mutations of splicing machinery in myelodysplasia. Nature 2011;478:64–9.
8. Yoshida K, Toki T, Okuno Y, Kanezaki R, Shiraishi Y, Sato-Otsubo A, et al. The landscape of somatic mutations in Down syndrome-related myeloid disorders. Nat Genet 2013;45:1293–9.
9. Gurtan AM, Lu V, Bhutkar A, Sharp PA. *In vivo* structure-function analysis of human Dicer reveals directional processing of precursor miRNAs. RNA 2012;18:1116–22.
10. Banerji S, Cibulskis K, Rangel-Escareno C, Brown KK, Carter SL, Frederick AM, et al. Sequence analysis of mutations and translocations across breast cancer subtypes. Nature 2012;486:405–9.
11. Network CGAR. Integrated genomic analyses of ovarian carcinoma. Nature 2011;474:609–15.
12. Network CGAR. Comprehensive genomic characterization of squamous cell lung cancers. Nature 2012;489:519–25.
13. Pugh TJ, Weeraratne SD, Archer TC, Pomeranz Krummel DA, Auclair D, Bochicchio J, et al. Medulloblastoma exome sequencing uncovers subtype-specific somatic mutations. Nature 2012;488:106–10.
14. Pugh TJ, Morozova O, Attiyeh EF, Asgharzadeh S, Wei JS, Auclair D, et al. The genetic landscape of high-risk neuroblastoma. Nat Genet 2013;45:279–84.
15. Ding L, Ley TJ, Larson DE, Miller CA, Koboldt DC, Welch JS, et al. Clonal evolution in relapsed acute myeloid leukaemia revealed by whole-genome sequencing. Nature 2012;481:506–10.
16. Nik-Zainal S, Van Loo P, Wedge DC, Alexandrov LB, Greenman CD, Lau KW, et al. The life history of 21 breast cancers. Cell 2012;149:994–1007.
17. Anglesio MS, Wang Y, Yang W, Senz J, Wan A, Heravi-Moussavi A, et al. Cancer-associated somatic DICER1 hotspot mutations cause defective miRNA processing and reverse-strand expression bias to predominantly mature 3p strands through loss of 5p strand cleavage. J Pathol 2013;229:400–9.
18. Suzuki HI, Yamagata K, Sugimoto K, Iwamoto T, Kato S, Miyazono K. Modulation of microRNA processing by p53. Nature 2009;460:529–33.
19. Lujambio A, Lowe SW. The microcosmos of cancer. Nature 2012;482:347–55.
20. Wang X, Zhao J, Huang J, Tang H, Yu S, Chen Y. The regulatory roles of miRNA and methylation on oncogene and tumor suppressor gene expression in pancreatic cancer cells. Biochem Biophys Res Commun 2012;425:51–7.

Grant Support

This work was supported by Research on Measures for Intractable Diseases, Health, and Labor Sciences Research Grants, the Ministry of Health, Labour and Welfare; Research on Health Sciences focusing on Drug Innovation; the Japan Health Sciences Foundation, grant from the Ministry of Education, Culture, Sports, Science and Technology of Japan, KAKENHI (22134006), the Project for the Development of Innovative Research on Cancer Therapeutics (P-DIRECT), and also by the Japan Society for the Promotion of Science through the "Funding Program for World-Leading Innovative R&D on Science and Technology (FIRST Program)," initiated by the Council for Science and Technology Policy.

The costs of publication of this article were defrayed in part by the payment of page charges. This article must therefore be hereby marked *advertisement* in accordance with 18 U.S.C. Section 1734 solely to indicate this fact.

Received August 27, 2013; revised February 17, 2014; accepted March 9, 2014; published OnlineFirst March 27, 2014.